5553

The influence of airflows on the hygro-thermal behaviour of sloped insulated roofs

case study of a hot box - cold box experiment

Arnold Janssens
Laboratorium Bouwfysica
Leuven, Belgium

IEA-Annex 24 HAMTIE
october 1991 .

0. INTRODUCTION

This paper is an interim report of a hot box - cold box experiment which has run at the Laboratory of Building Physics, KU Leuven, from januari to june 1991 on sloped roofs, with full insulation-filling in the sides. The first part describes the measuring method. Three different lay-outs were studied: the first with a capillary-porous, hygroscopical underroof underneath the tile-deck, the second without an underroof and the third with a non-capillary, vapour- and air-tight underroof. The experiment was developed in three stages, during which the element 'convection' played a more and more important role.
The second part describes the results: temperatures- and heatflow-profiles and weight-increase of the separate construction parts, and compares the differences between the three lay-outs. The phenomena influencing the thermal and hygric behaviour of the roofs are analysed.

Further steps in the research are to compare the found values with the ones predicted in simulations, to analyse the differences between measured and calculated values and to take a look at energetical consequences.

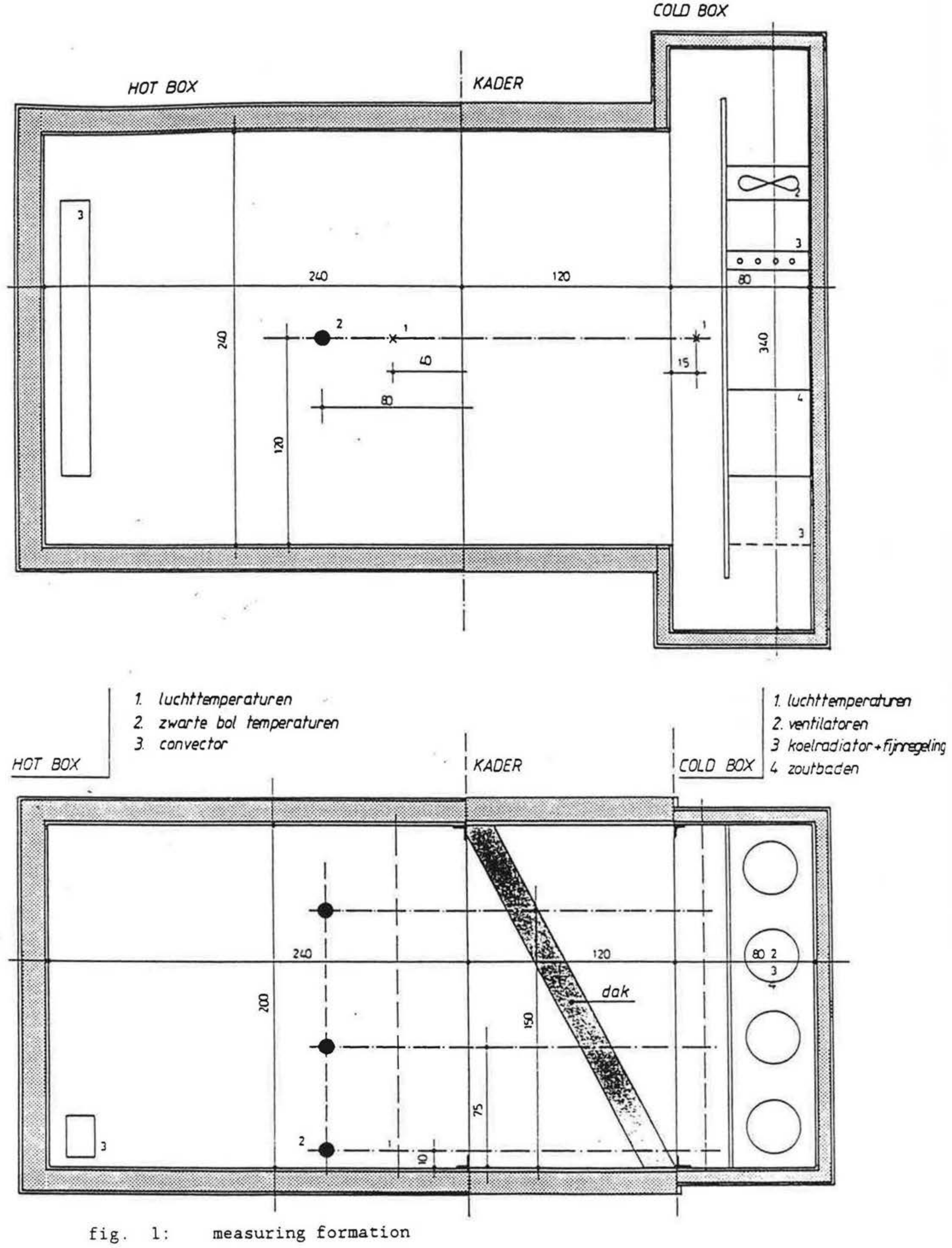

fig. 1: measuring formation

1. MEASURING METHOD

a. Measuring formation (fig. 1)

* *Cold Box:*

- inner dimensions lxbxh = 3.4 x 0.8 x 2.0 m;
- envelope construction: sandwich "multiplex 22 mm, XPS 60 mm, multiplex 22 mm", thermal resistance R = 2.67 $W/(m^2.K)$;
- the cold box is painted black on the inside (long-wave emissivity e = 0.9), and is divided into two parts by a radiation screen (emissivity e = 0.9); behind this screen, following instruments are installed: a fan-group, a cooling radiator with external unit and a heating element for precision control; they establish a homogeneous air-temperature distribution and a sufficient air-velocity (± 4 m/s) in the measuring zone of the cold box; a constant relative humidity is realised by installing some baths with an unsaturated salt solution (NaCl in this case);
- in the cold box the outside climate is simulated.
- *measuring points:*
  - air-temperatures and air-pressures in the middle of the measuring opening, at a depth of 15 cm and at a height of resp. 10 cm, 70 cm and 150 cm;
  - relative humidity at a depth of 15 cm and at a height of 150 cm.

* *Hot Box:*

- inner dimensions lxbxh = 2.4 x 2.4 x 2.0 m;
- envelope construction: sandwich "multiplex 22 mm, XPS 120 mm, multiplex 22 mm", thermal resistance R = 4.98 $W/(m^2.K)$;
- the hot box is painted black on the inside (long-wave emissivity e = 0.9), and is heated by a convective heating element, placed in the back; a constant relative humidity is realised by installing some baths with a saturated salt solution ($Mg(NO_3)_2$ in this case);
- the hot box can be connected to a fan-group, which blows air from the laboratory to the hot box and creates an air-pressure difference over the testing construction.
- in the hot box the inside climate is simulated.
- *measuring points:*
  - air-temperatures and air-pressures in the middle of the measuring opening, at a depth of 40 cm and at a height of resp. 10 cm, 75 cm and 150 cm;
  - relative humidity at a depth of 40 and at a height of 150 cm.
  - black globe temperatures at a depth of 80 cm and at a height of resp. 10 cm, 75 cm and 150 cm.

* *Measuring Frame, in which the testing roof is fixed:*

- inner dimensions lxbxh = 1.25 x 2.35 x 2.00 m;
- envelope construction: "multiplex 22 mm, XPS 120 mm", R = 5.40 $W/(m^2.K)$.

The Hot Box / Cold Box measuring formation is placed in a non-conditioned laboratory, heated by blown air.

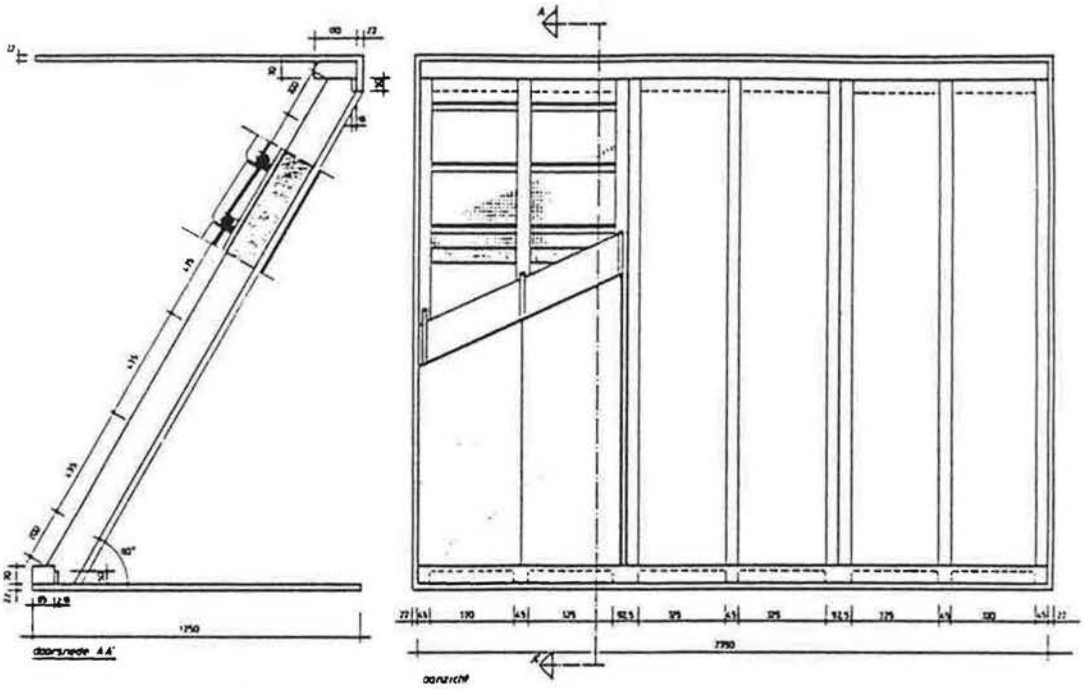

fig. 2: Measuring frame; construction

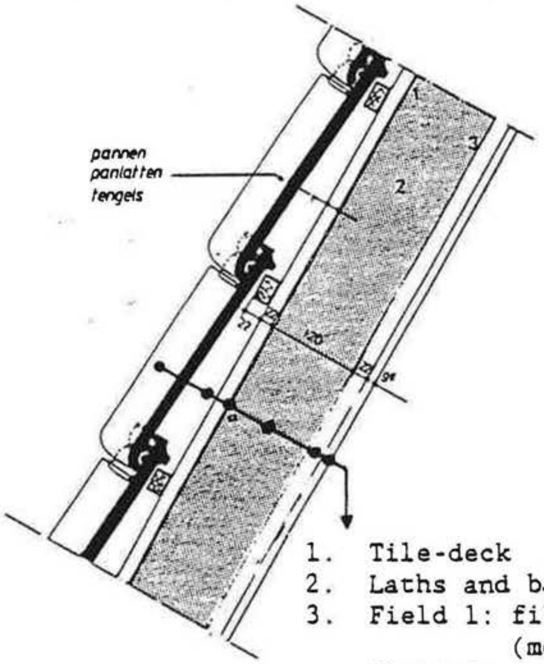

1. Tile-deck
2. Laths and battens
3. Field 1: fibre-cement board underroof (menuiserite)
   Field 2: no underroof
   Field 3: DFOL-SPS PE-foil underroof
4. Isover uniroll roof-insulation
5. Wiring cavity
6. Gypsum board

fig. 3: Roof section

b. Testing Roof

** Construction: (fig. 2)*

The roof is divided into 3 different fields, each constructed as a fragment (lxb = 2.14 m x 0.78 m) of a woodframe roof, insulated between the rafters: roof slope = 60°; section of rafters = 45 mm x 120 mm; distance between centerlines = 367 mm. The fields are separated from each other by a double rafter with a vapour-tight bituminous layer in between. The 3 fields are referred to as Field 1, Field 2 and Field 3. The different parts of the roof-section are conceived to be detachable, in order to be able to follow their weekly change of weight.

** Section of Field 1 (inside to outside): (fig. 3)*

- gypsum board, d = 9.5 mm; joints (edges) are closed with silicons;
- air (wiring) cavity, d = 22 mm;
- glass-wool insulation, ISOVER-UNIROLL, d = 120 mm; half of the insulation can be taken out for weighing;
- frame with underroof: fibre-cement cellulose board (menuiserite), d = 3.2 mm; the board is assembled in two parts with an horizontal overlap (= 40 mx), situated at 1.2 m from the bottom edge, and is fixed on a wooden frame (22 mm x 36 mm); this frame is attached on the underlying rafters by means of bolts and nuts;
- 1 batten, 22 mm x 36 mm, dismountable;
- 8 tile laths, 22 mm x 36 mm, dismountable;
- 36 glazed tiles (8 rows of 4), double lock type, dismountable.

** Section of Field 2:*

- the same as Field 1, except that no underroof is fixed in the wooden frame.

** Section of Field 3:*

- the same as Field 1, except that another underroof is fixed in the wooden frame: type D-Foil-SPS, glass fabric reinforced, micro-perforated PE-foil, d = 0.2 mm; the foil is assembled in two parts with an horizontal overlap = 100 mm, situated at 1.2 m of the bottom edge.

** Measuring points, per field: (fig. 4)*

- temperatures on each layer-surface;
  measured at 5 heights on both sides of the insulation (at 20.0, 63.5, 107.0, 150.5 and 194.0 cm from the bottom edge, measured along the slope);
  measured at 3 heights on both surfaces of gypsum-board, underroof (for field 1 & 3) and tiles (at 20.0, 107.0 and 194.0 cm from the bottom edge, measured along the slope);
- air-pressures in the wiring cavity between gypsum-board and insulation, inbetween insulation and underroof (for field 1 & 3) and in the cavity under the tiles; additional air-pressures are measured on the tiles of field 2, taken as the reference pressure in the Cold Box;
  measured at 3 heights: 20.0, 107.0 and 194.0 cm:
- heatflow densities on both sides of the insulation, measured at 3 heights: 20.0, 107.0 and 194.0 cm.

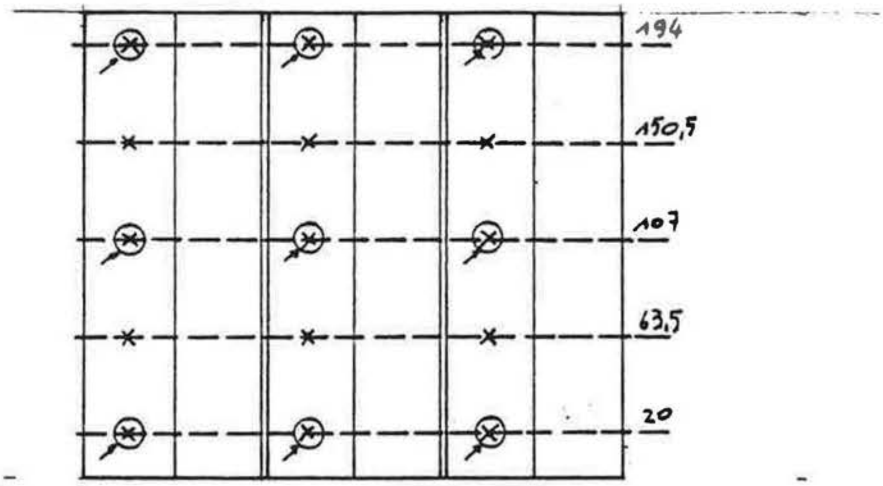

On the insulation layer

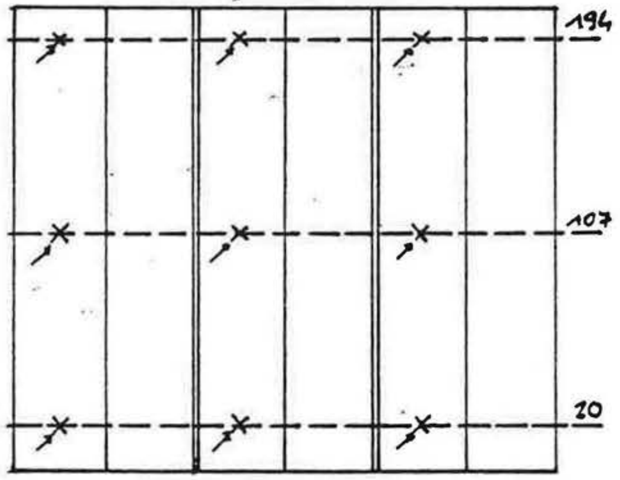

On other layers

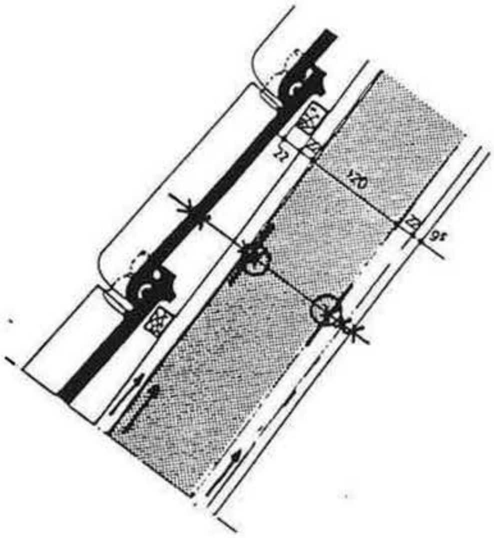

fig. 4: Measuring points:
- x thermocouples
- o heatflow sensors
- ↗ pressure tubes

c. Measuring equipment

- temperatures: Cu-Konst thermocouples;
- heatflow densities: TNO-WS 31 heatflow-sensors (d = 10 cm);
- air-pressures: PE pressure-tubes (d_i = 3 mm);
- relative humidity: Capacitive hygrometers.

The thermo-couples are connected with a HP-3497A 100 canals-logger, the heatflow-sensors and hygrometers with a HP-3421A 20 canals-logger. Both loggers are conducted by a Commodore PC-10.
Air-pressures are measured with a FC012-micromanometer.

d. Measuring course

** Temperatures, heatflows and relative humidity*
These are continuously measured by the computer by scanning the logger-canals each 15 minutes, during a whole week. The output consists of the weekly averaged values and deviations of measured temperatures, heatflow densities and relative humidities.

** Air-pressures*
These are measured at the end of each week.

** Moisture migration and condensation*
Moisture migration through the construction is weekly mapped by weighing all the composing parts of the three roof-sections.
At the end of each week, the boxes are opened, the roofs are disassembled and tiles, laths, battens, underroofs, insulation and salt-baths are weighed. The whole operation (from the opening till the closing of the boxes) takes about 2 hours.

e. Measuring development

The experiment is developed in 3 stages, during which the convection-element becomes more important.

* *STAGE 1: diffusion*
  . duration: 8 weeks;
  . a constant temperature- and vapour pressure-difference is installed between hot and cold box.

* *STAGE 2: diffusion-convection, air-tight construction*
  . duration: 5 weeks;
  . a constant temperature-, vapour pressure- and air-pressure-difference is installed between hot and cold box.

* *STAGE 3: diffusion-convection, air-open construction*
  . duration: 13 weeks;
  . a constant temperature-, vapour pressure- and air-pressure-difference is installed between hot and cold box;
  . stage 3 is divided into 3 levels:
    - *STAGE 3a:* (4 weeks) the roofs are made air-open by sawing 2 horizontal grooves (width = 0.4 cm, length = 78.0 cm) in the gypsum board, at 60.0 cm from the bottom and from the top (measured along the slope), simulating the placing of plaster board with open joints;
    - *STAGE 3b:* (4 weeks) same as 3a, except that 2/3 of the grooves is closed with tape, leaving 2 horizontal grooves (width = 0.4 cm, length = 26.0 cm);
    - *STAGE 3c:* (5 weeks) same as 3b, except that in the hot box the $Mg(NO_3)_2$-baths are replaced by H_2O-baths, creating a bigger vapour pressure-difference.

2. RESULTS

a. Boundary conditions (fig. 5 - 8)

** Temperature, vapour pressure, relative humidity*
From the moment that the fan-group is connected to the hot box, the temperature- and vapour pressure-course become less stable: the temperature in the hot box reacts quickly to temperature-variations in the laboratory. With increasing airflow-rate (stage 2 - 3), the relative humidity in the hot box falls while the relative humidity in the cold box rises: by convection, more moisture is transported through the construction. As a consequence, the vapour pressure-difference drops during stage 2, 3a and 3b.

** Air-pressure*
When comparing the hygro-thermic behaviour of the 3 roof-sections, it is important to know that the air-pressure-differences differ from field to field and depend on the height.
This is due to a complex pressure field in the cold box on the tiles of the roofs. The fan-group in the box creates an air-flow moving from field 1 to field 3 creating dynamic pressures: the irregular shape of the flow-section explains the large differences over the pressure field. Measurement of the air-pressures on the outside surface of the tiles and on the inside surface of the gypsum-board during stage 1, learns that even then we're not looking to "pure diffusion" only, and that we have to take convection into account (fig. 9).

Table 1: measured air-pressures (Pa) during stage 1 "diffusion"

PLACE		height (cm): 20	107	194
FIELD 1	HB	-0.7	-0.6	-0.6
	CB	-2.0	-3.2	-1.8
FIELD 2	HB	-0.8	-0.7	-0.6
	CB	-4.0	-3.0	-3.5
FIELD 3	HB	-0.7	-0.6	-0.6
	CB	0.5	0.5	-1.0

In field 1 the air-pressure on the tiles is the lowest in the middle of the roof, and becomes higher to the bottom and the top; averaged air-pressure difference $\Delta p_a = 1.7$ Pa.
In field 2 the air-pressure on the tiles is the highest in the middle of the roof, and becomes lower to the bottom and the top; $\Delta p_a = 2.8$ Pa.
In field 3 the air-pressure on the tiles becomes lower from top to bottom; $\Delta p_a = -0.6$ Pa, inducing a cold air-flow, moving from cold to hot box, opposite to the one induced in field 1 and 2.
For the interpretation and simulation of the hygro-thermic behaviour of the roofs, we assume the differences in air-pressure between the fields to be the same during the 3 stages.

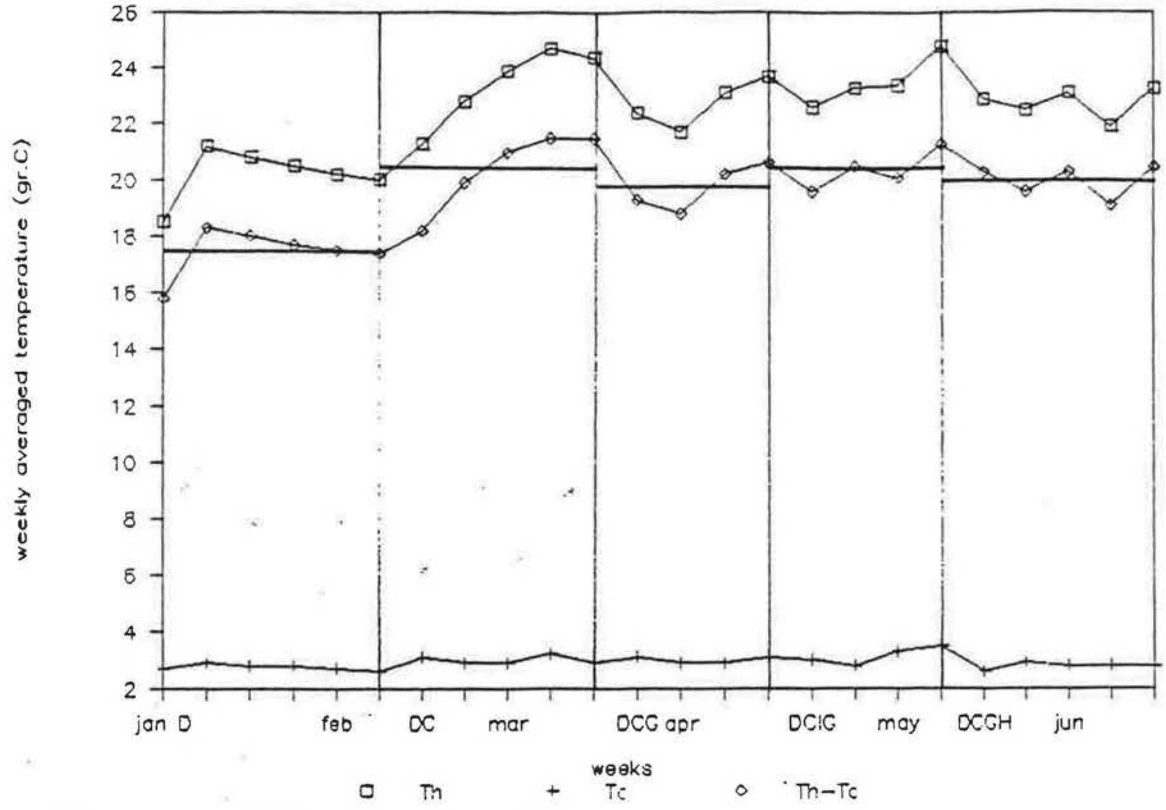

fig. 5: temperature vs time

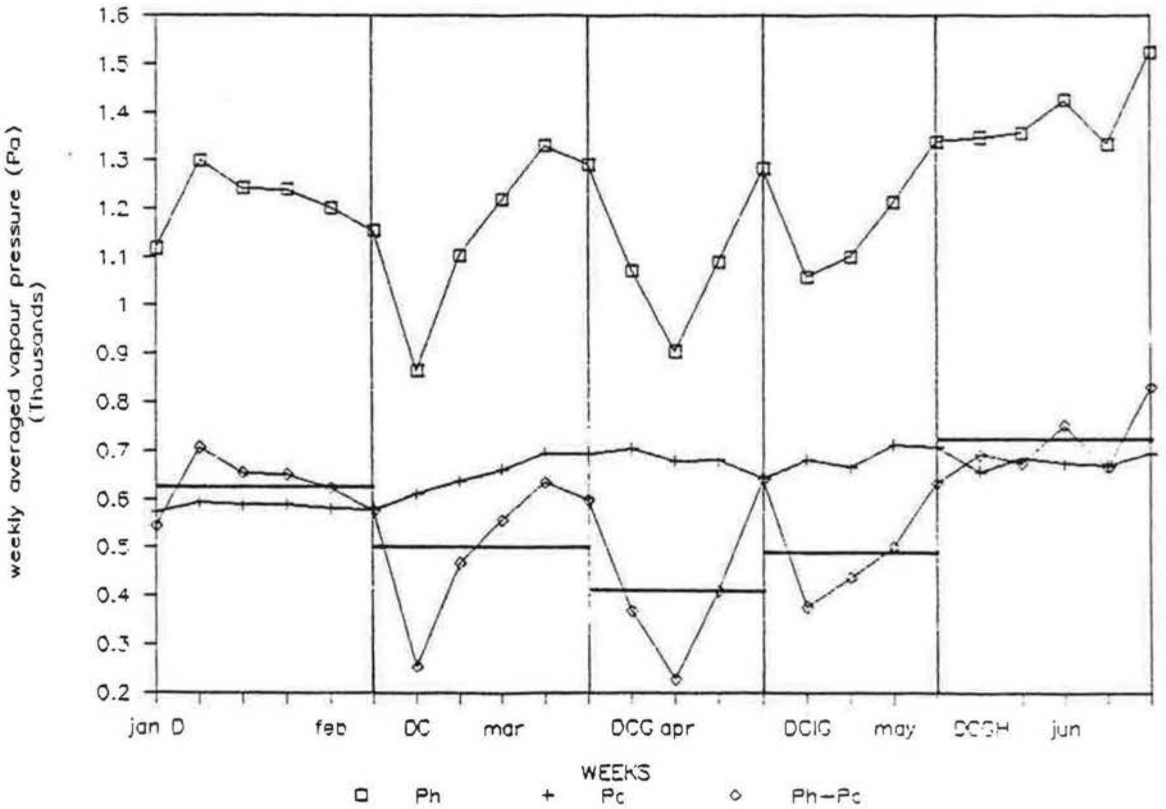

fig. 6: vapour pressure vs time

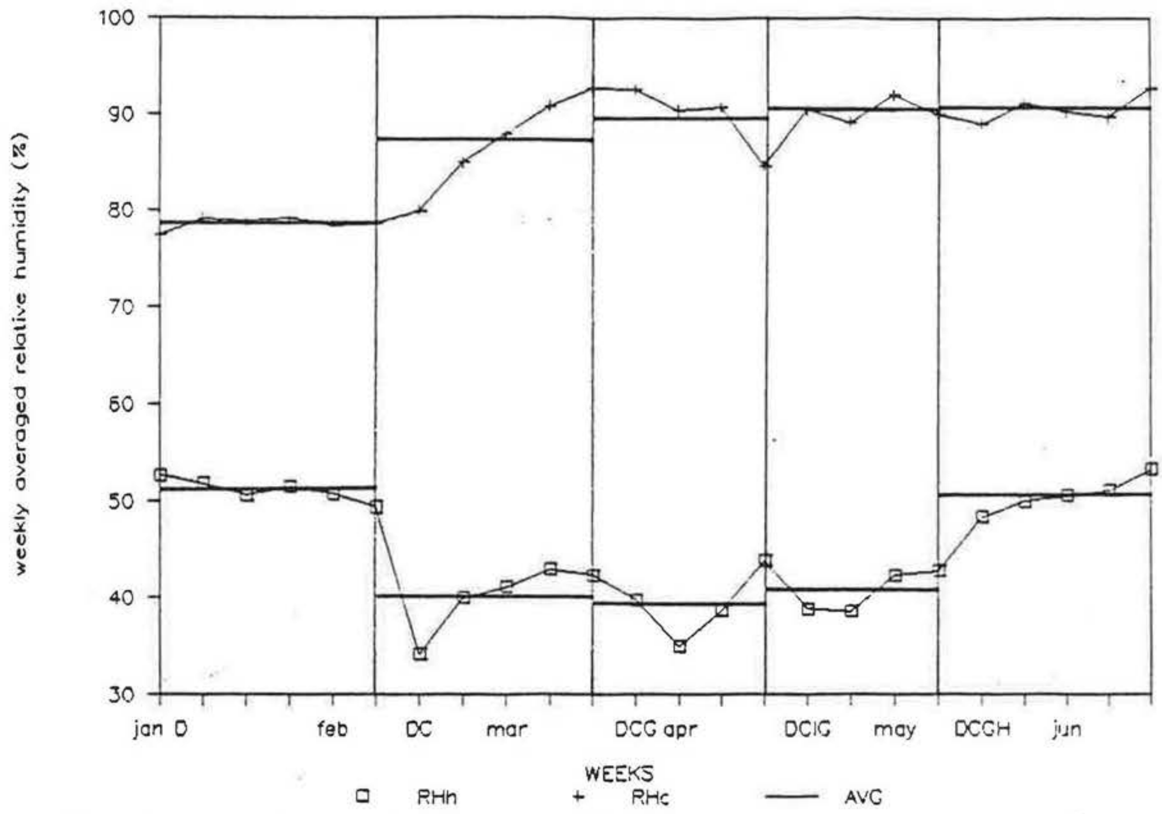

fig. 7: relative humidity vs time

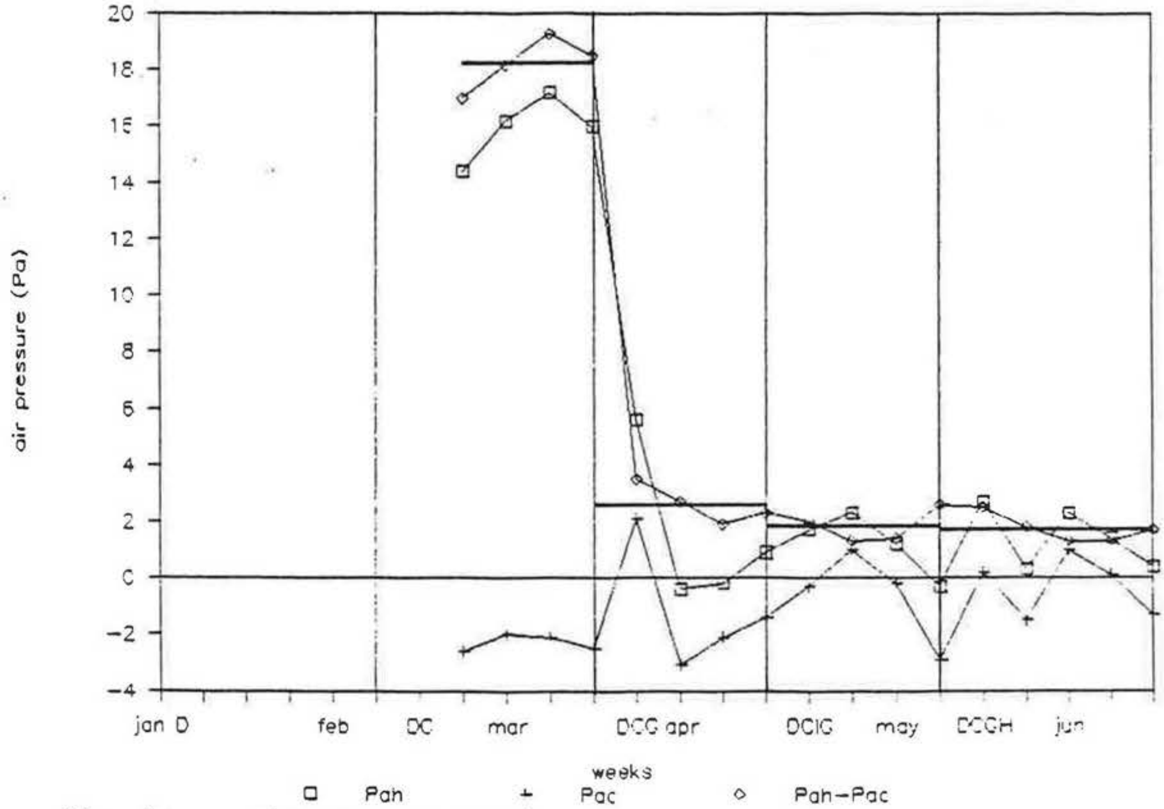

fig. 8: air-pressure vs time

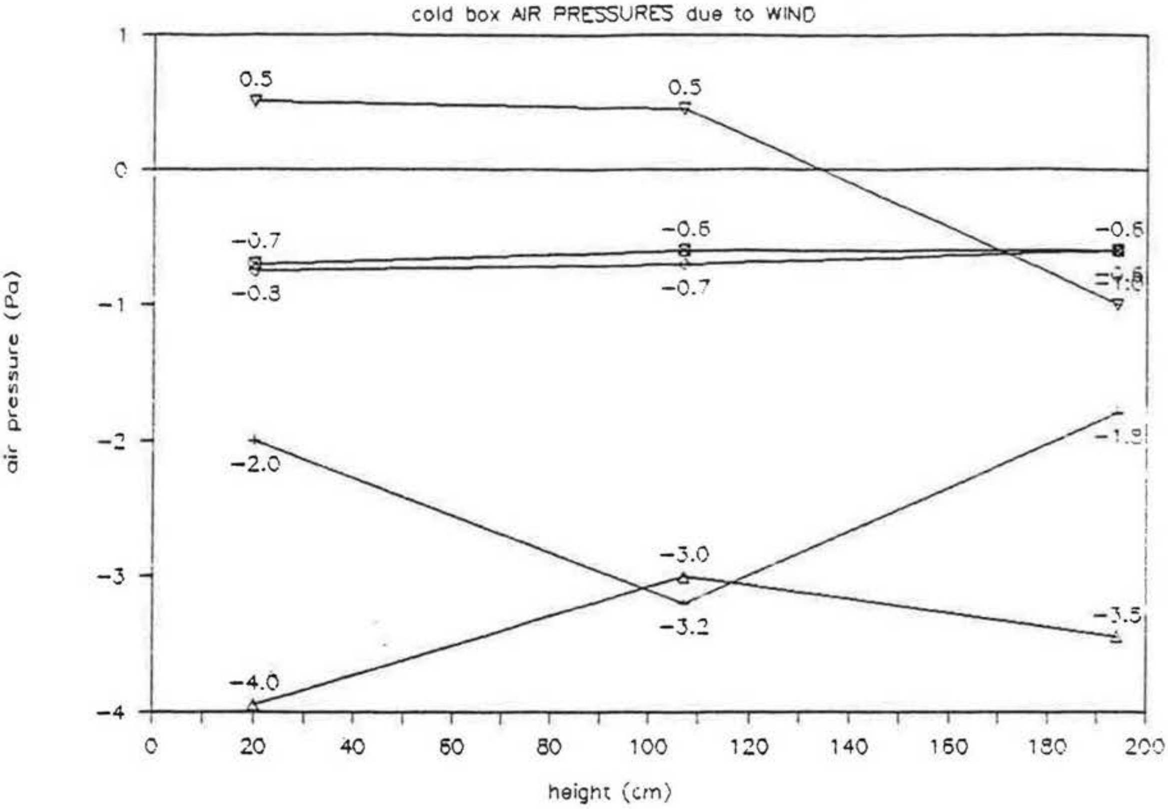

fig. 9: air-pressure vs height; STAGE 1 'diffusion'

- □ field 1: inside surface (gypsum board)
- + field 1: outside surface (tiles)
- ◇ field 2: inside surface (gypsum board)
- Δ field 2: outside surface (tiles)
- x field 3: inside surface (gypsum board)
- ∇ field 3: outside surface (tiles)

b. Temperatures (fig. 10 - 14)

The figures show the averaged values of the measured temperatures per stage. These temperature-profiles give an indirect picture of the complex way air moves in and through the roofs, caused by following effects:

* *Natural convection*

Natural convection is directly linked to air density differences, induced by temperature differences and resulting in rotative stack flow in and around the insulating layer: air is warmed up at the inner side of the insulation layer, rises along the warm surface and infiltrates through the insulation to the cold side, causing higher temperatures at the top of the outside surface of the insulation. Here the air cools down again, drops along the cold surface, and flows back to the warm side, causing locally lower temperatures.

The temperature-effect caused by the stack flow is clearly present during all the stages of the experiment, although it is sometimes influenced or diminished by a local change in geometry or by the results of forced convection.

* *Forced convection*

Forced convection is linked to air pressure differences and to a lack of air tightness. Convective air flows change the temperature-fall through a construction from a linear to an exponential one: this results in small temperature-gradients on the inside of the insulation layer and in large gradients on the outside of the insulation - in case of a positive global airflow rate: moving from in- to outside. The opposite happens in case of a negative airflow rate. The more air-open a construction and the bigger the airflow through it, the stronger the influence on the temperature-gradient becomes.
Forced convection also diminishes the effects of stack flow, without ever canceling it: air-velocities through the insulation layer are 'equalized' along the height of the construction. This is also stronger for more air-open constructions.

Both effects are present in the temperature profiles. During stage 3 the grooves, made in the gypsum board, result in a high air-openess of the roofs and in bigger airflow-rates then before. Even the air-pressure difference of 18 Pa during stage 2 couldn't establish a higher flow-rate through the air-tight roofs, then the pressure difference of 2 Pa during stage 3 (in field 1 & 2).
The effects are clear: in field 1 & 2 the temperatures of the gypsum board and at the warm surface of the insulation are equal to those in the hot box, while the temperatures of the layers on the cold side of the insulation (underroof and/or tiles) differ largely. This is stronger in field 2, being more air-open (no underroof) and submitted to a bigger air-pressure difference then field 1. The opposite is measured in field 3, where a negative airflow exists: here the temperatures of the layers on the warm side of the insulation diverge. Because field 3 is the most air-tight (PE-underroof), this effect, however, is less pronounced.

That also explains why only in field 3 the stack flow effects are still present during stage 3; in field 1 & 2 the temperature-gradient along the insulation surfaces disappears allmost completely. The temperature increase at the top of the cold side of the insulation, can also be caused by a local change in geometry.

** Geometry*

Air-density and air-pressure differences do not result in homogeneous airflow fields. Air-flows search the easiest way to move into and out of a construction. Therefore convective (both thermic as hygric) effects can be very local and concentrated at the most air-open parts of a construction or layer (leaks, grooves, overlaps). In the temperature-profiles these parts are easily identified.

In field 1, the local increase of temperature at the centre of the outside insulation surface, is caused by the overlap in the underroof (at 120 cm) to which the air-flows are directed. This peak is even more pronounced during stage 3, where the air is nearly pressed through the leaks in the underroof. This also explains the increase of temperature at the top and bottom of the same plane: here the joints 'underroof - measuring frame' are situated, introducing a horizontal leak (at 0 and 210 cm).
In field 2, during stage 3, the air is pressed through the grooves in the gypsum board (at 60 and 150 cm), and finds no resistance behind (the tile-deck being very air-open). This is clearly pronounced in the local temperature-peak at 60 and 150 cm.

** Cold box dynamic pressures*

As already stated, the 'wind' in the cold box creates a complex dynamic pressure-field, not only causing diverging (averaged) air-pressure differences over the separate fields (resulting in negative air-flows in field 3 during stage 1 & 3), but also causing intensive mixing of cold box air and the air in the 'underroof - tiles' cavity, by local airflows around each tile. This explains why the temperatures on both sides of the tiles stay in the same range during all stages.
These pressure gradients along the tile-deck also cause possible flows infiltrating from the cold box in the construction and back to the cold box. The temperature drop at the centre of the layers on the cold side of the insulation in field 2, might be explained by such a local cold box flow: pressure measurements revieled a higher pressure in the middle of the tile-deck (see "2a. Boundary conditions").

fig. 11: STAGE 1
temperature-profiles
heatflow-profiles

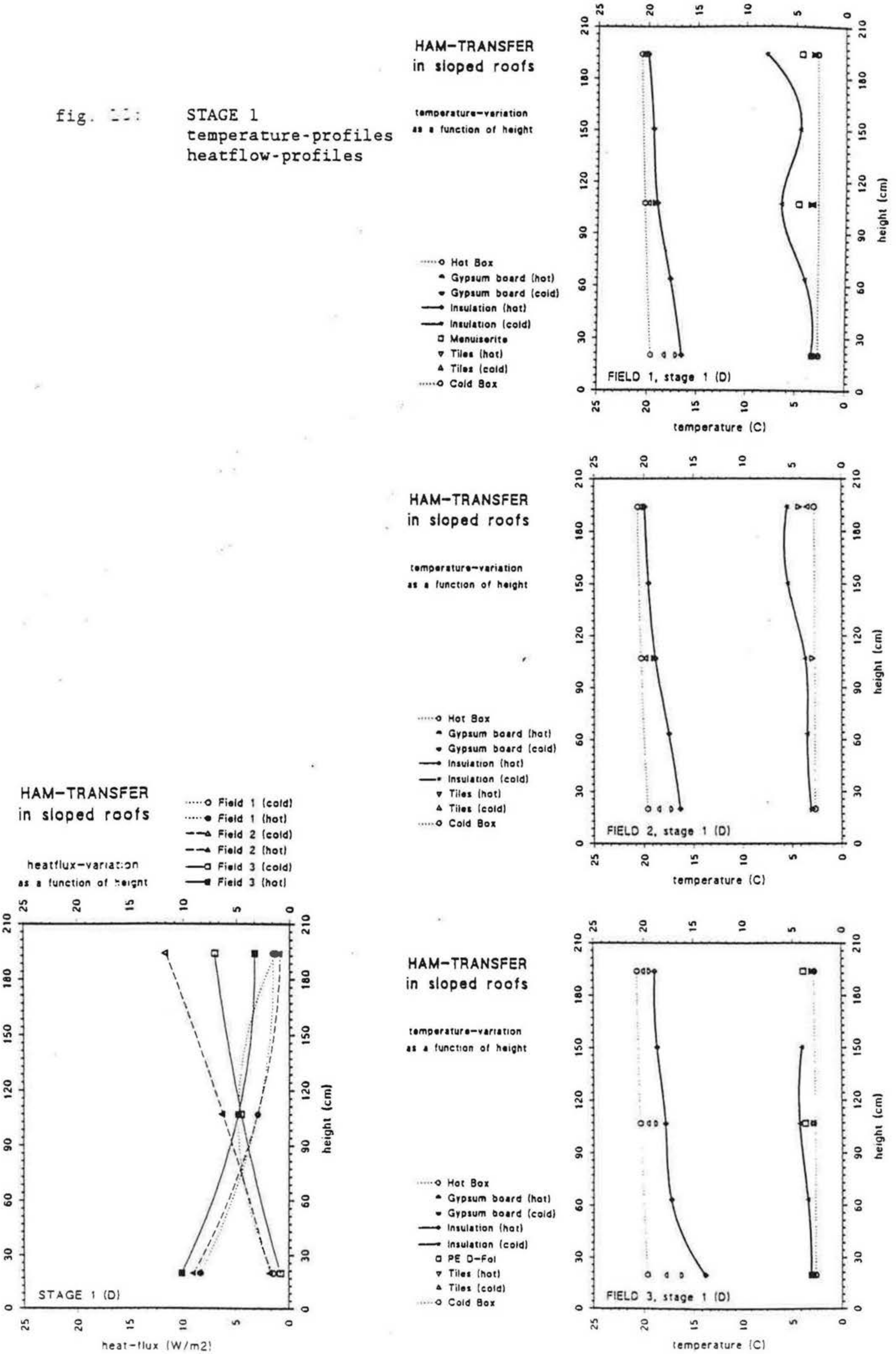

fig. 11: STAGE 2
temperature-profiles
heatflow-profiles

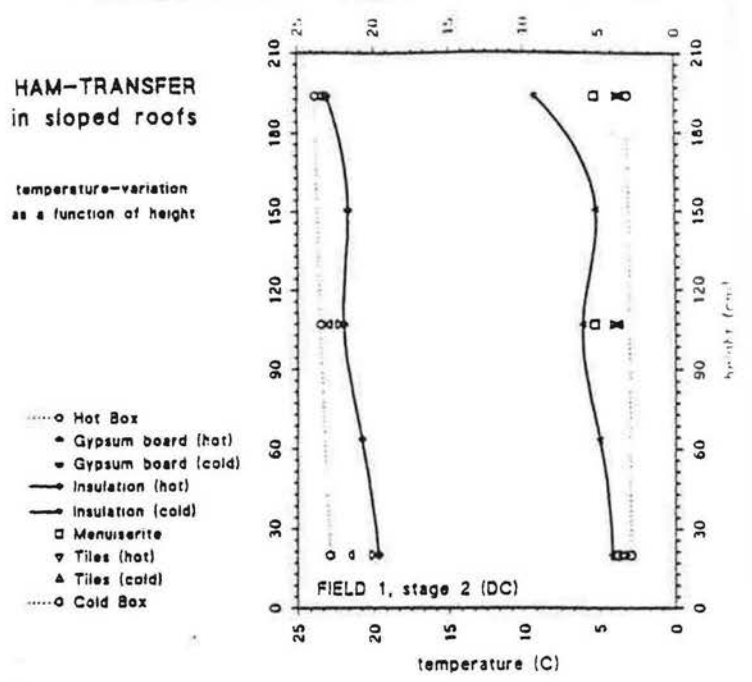

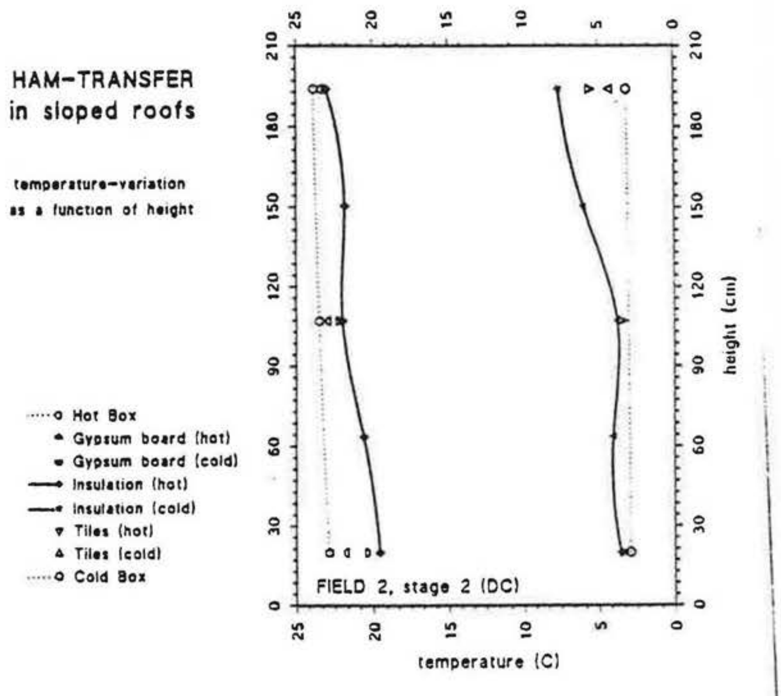

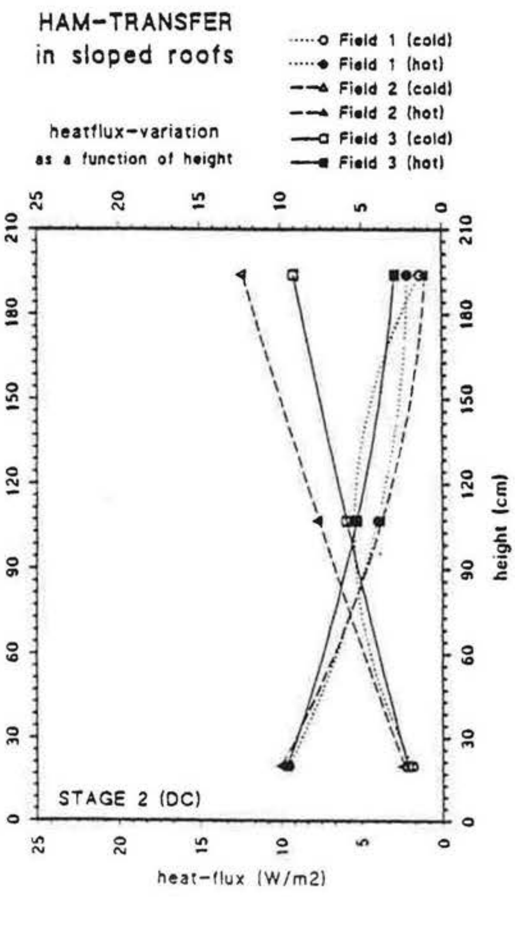

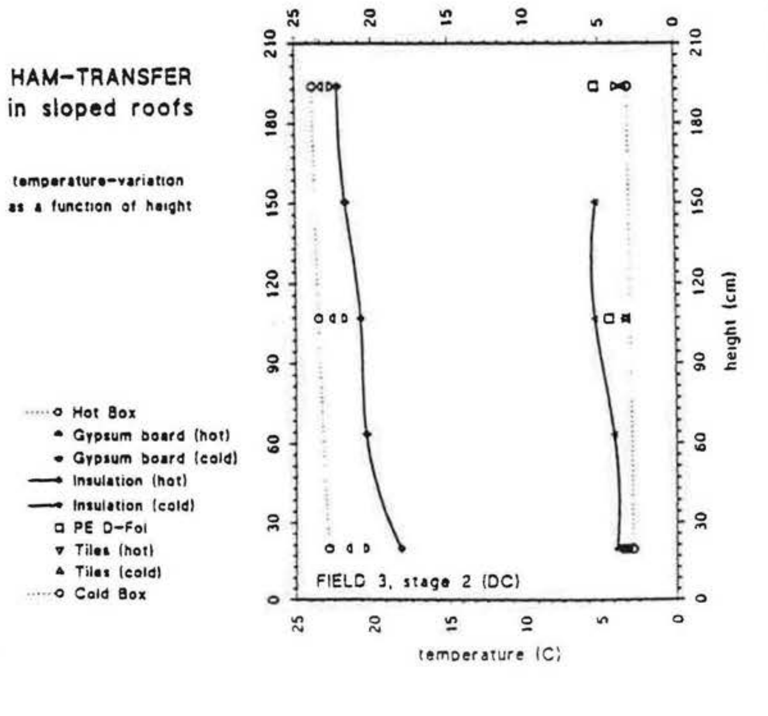

fig. 12: STAGE 3a
temperature-profiles
heatflow-profiles

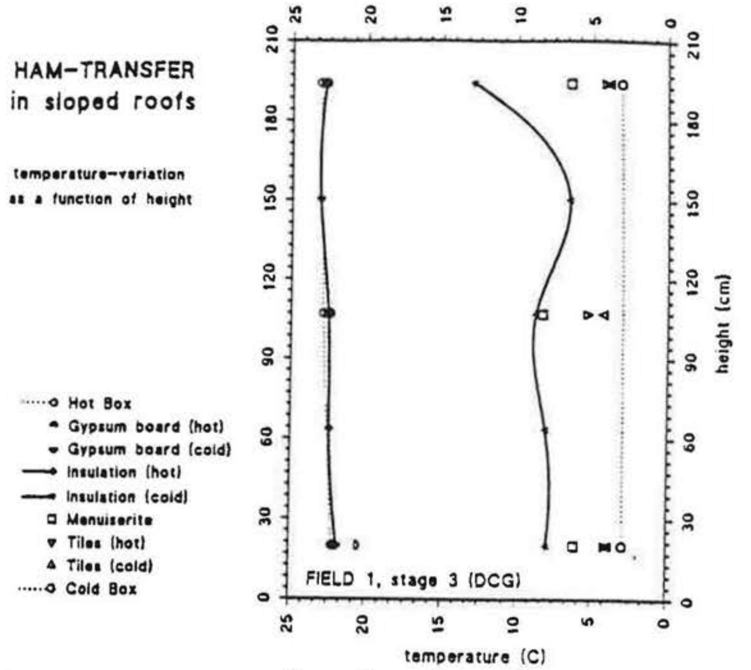

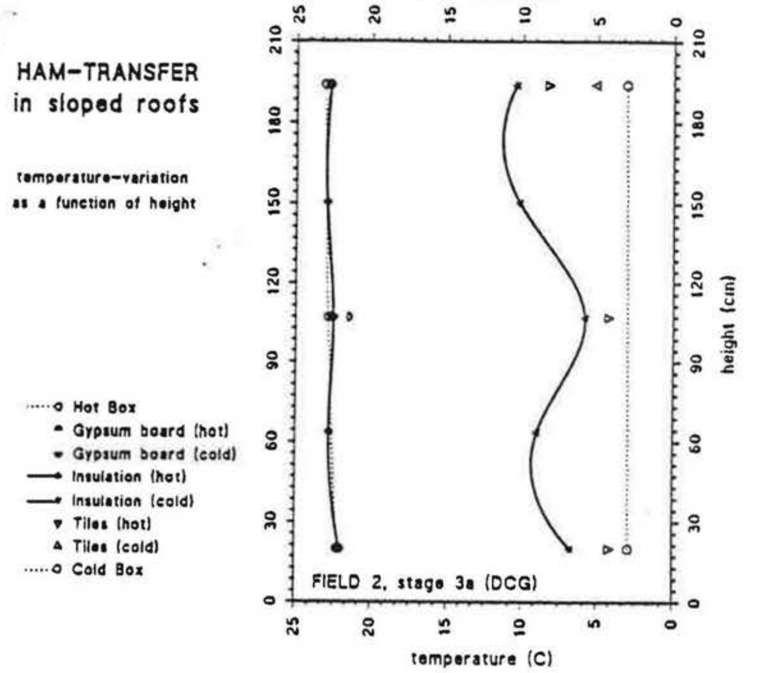

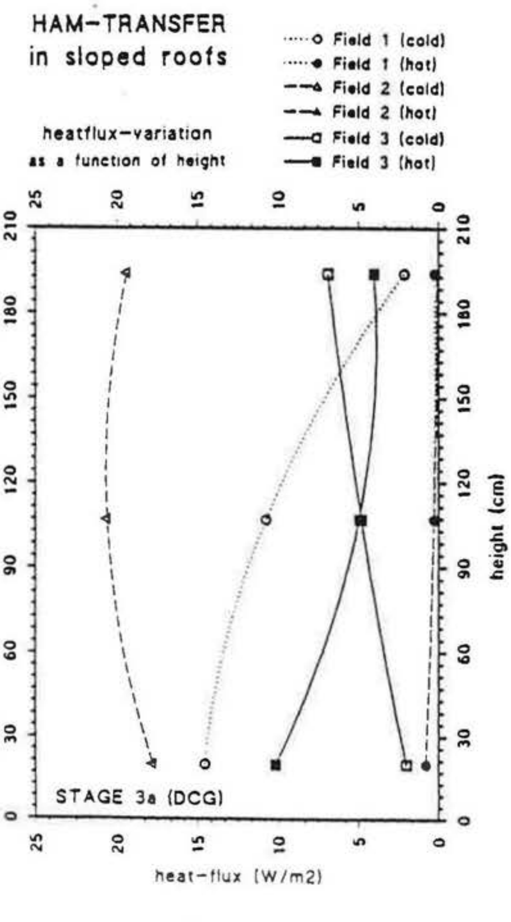

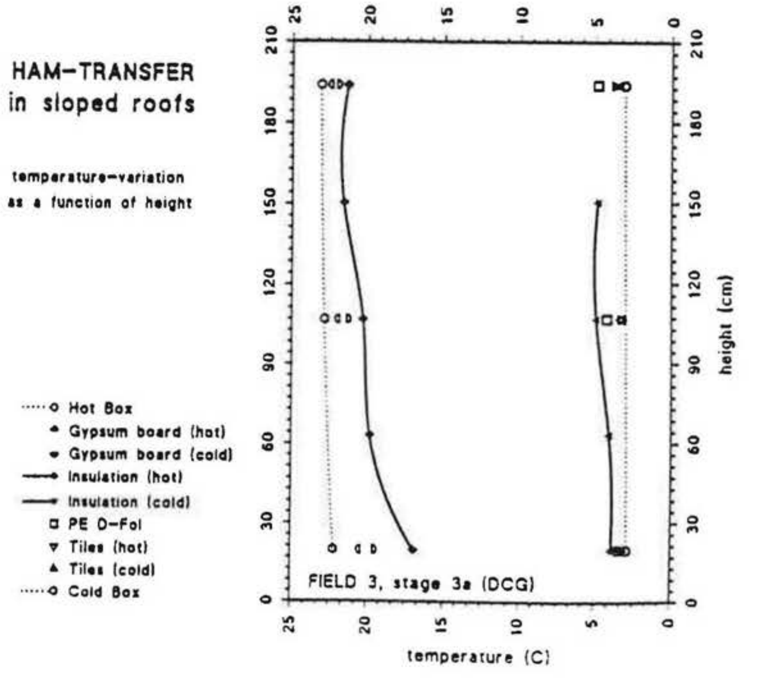

fig. 13: STAGE 3b
temperature-profiles
heatflow-profiles

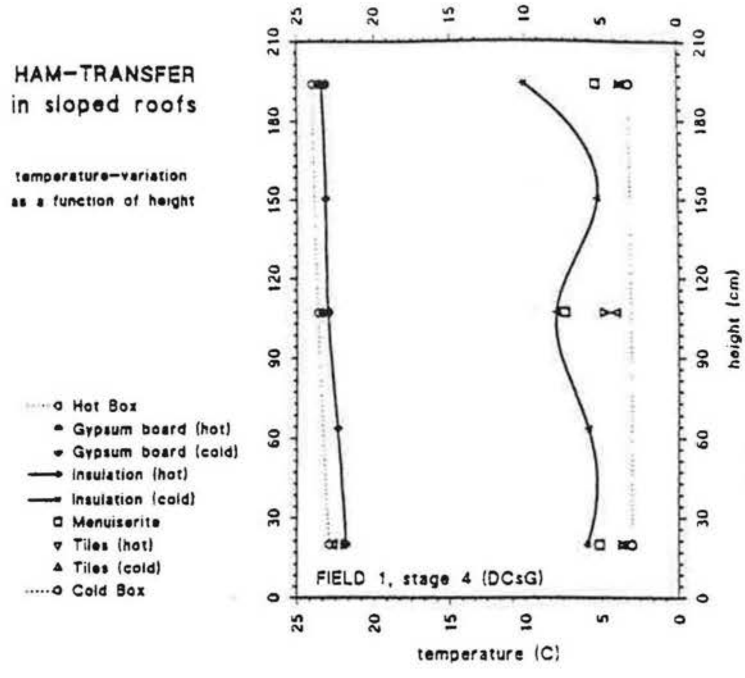

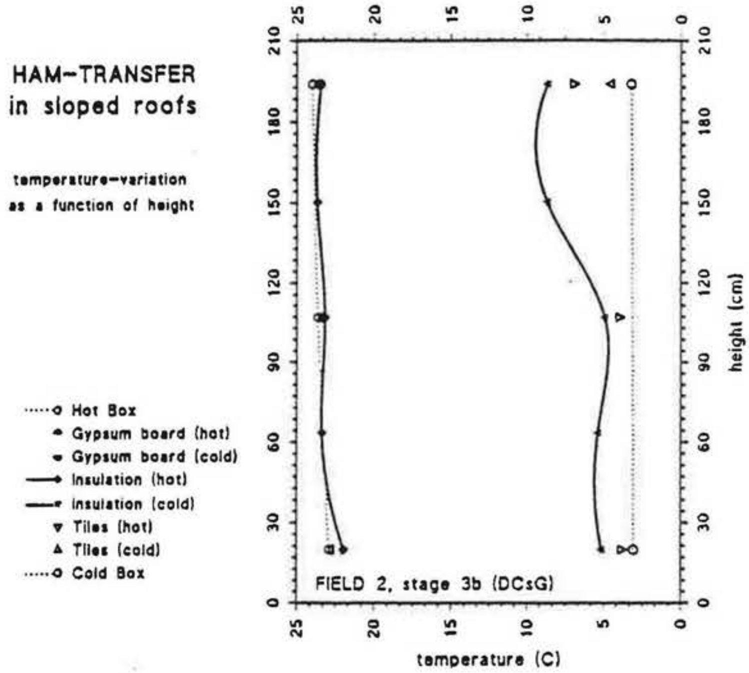

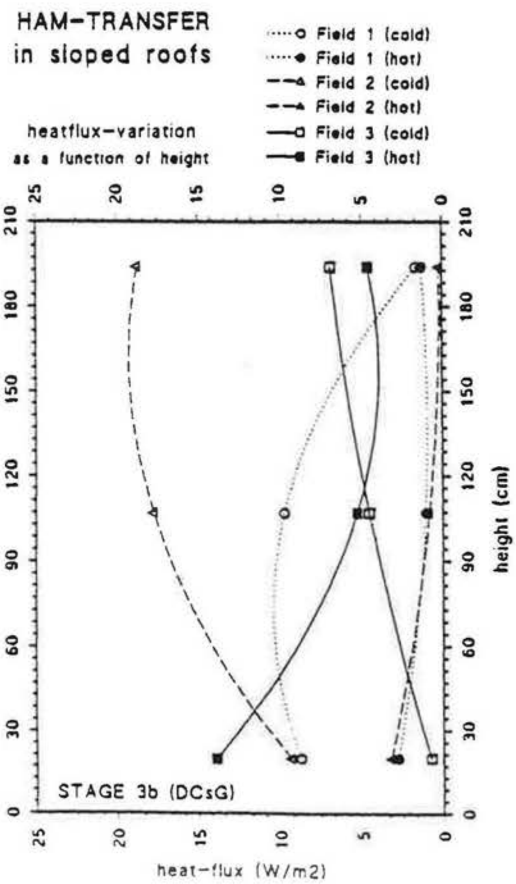

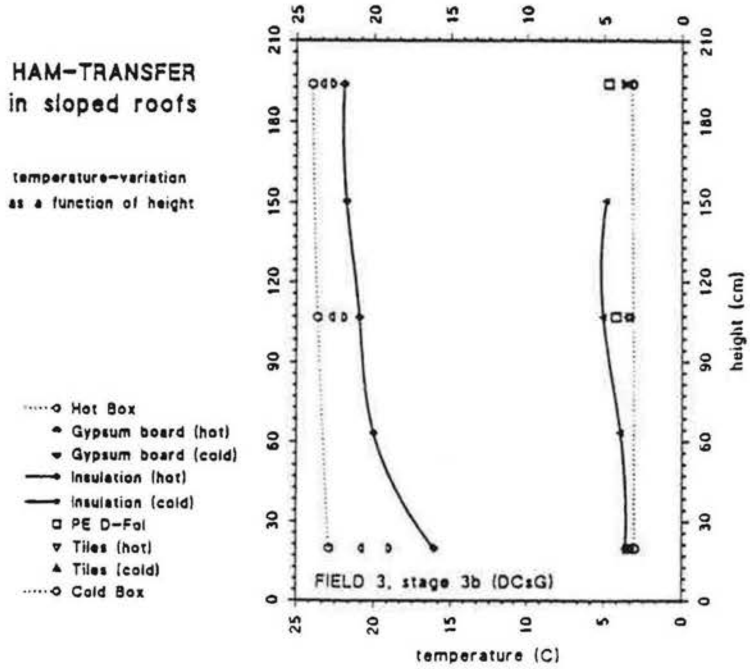

fig. 14: STAGE 3c
temperature-profiles
heatflow-profiles

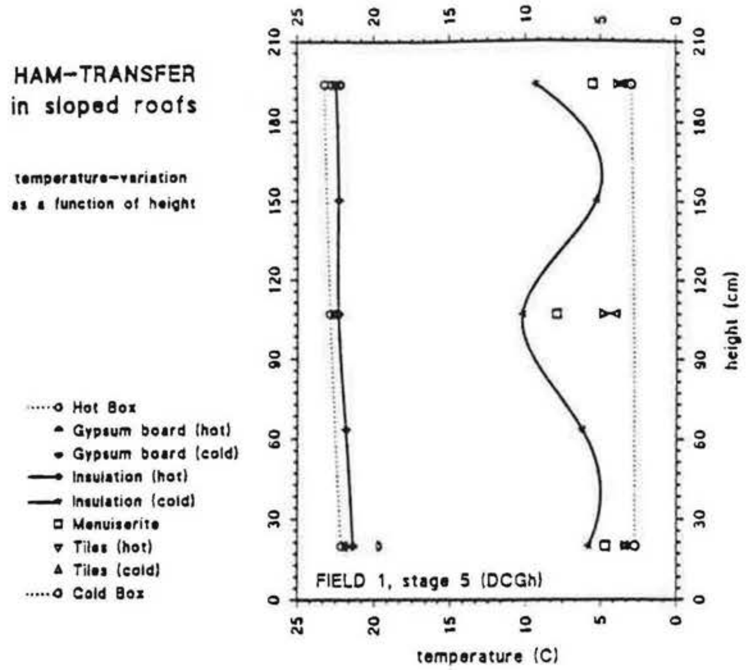

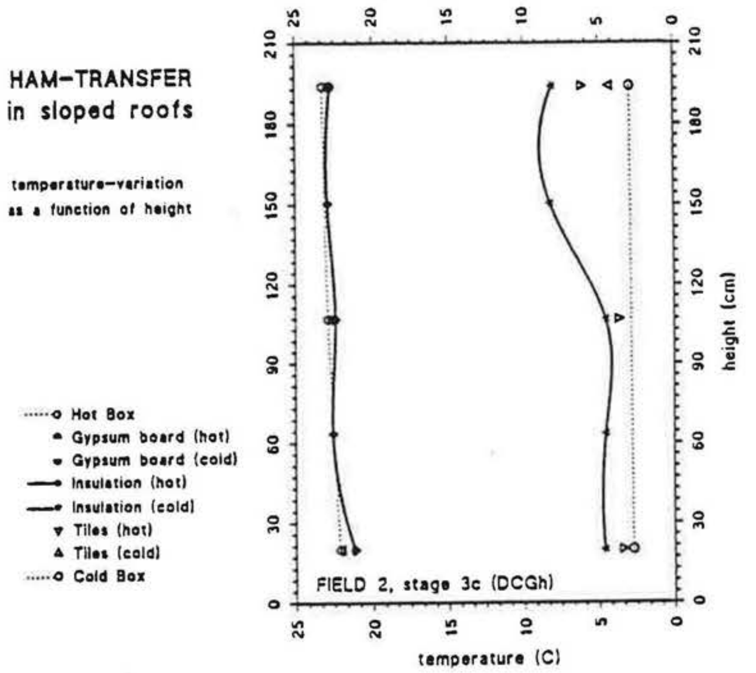

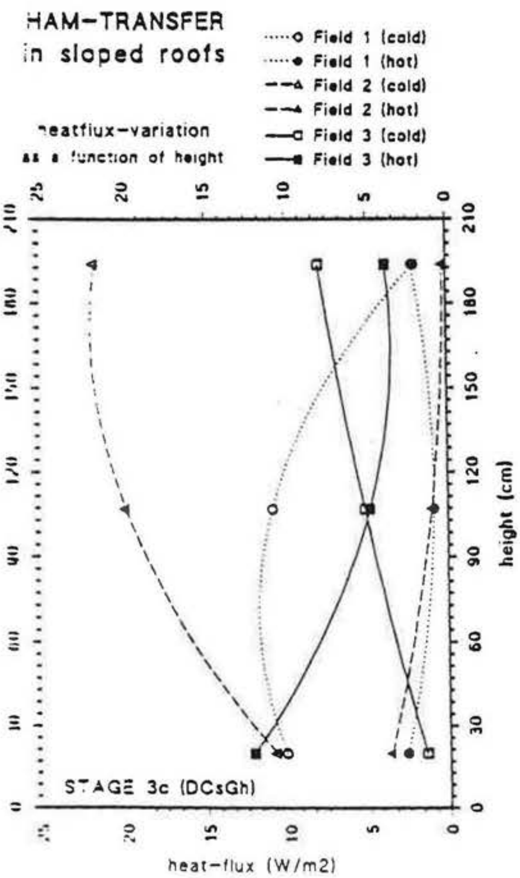

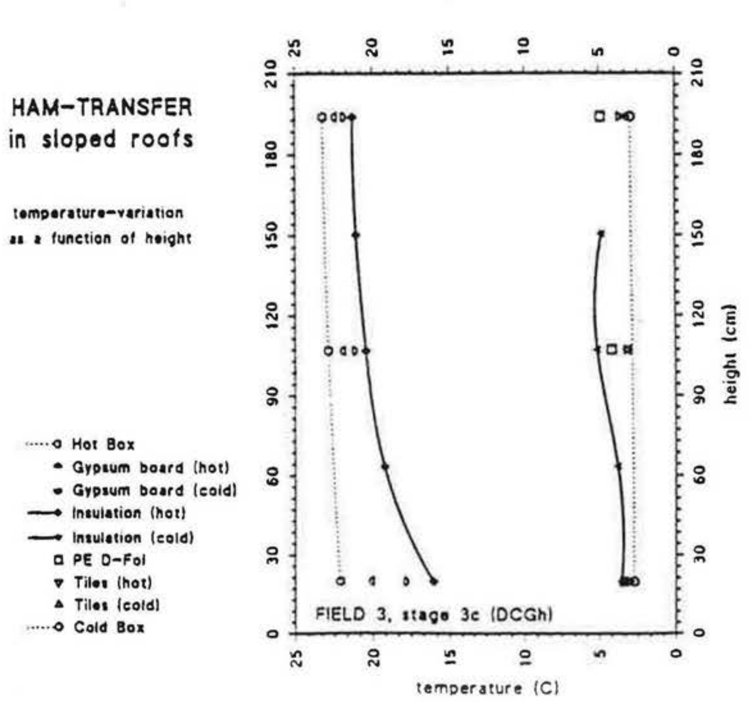

c. Heatflow densities and local air velocities

** Heat flow densities (fig. 10 - 14)*

Heat flow sensors measure a signal proportional to the local temperature-gradient. By calibrating them, the local conductive heat flow density can be derived. The conduction law (1-dimensional) states:

$$q_{cond} = -\lambda . \frac{\partial T}{\partial x} \qquad [1]$$

When air flows through a construction (no matter wether it is induced by temperature- or by pressure-differences), the temperature-fall over the section, changes from a linear to an exponential one, making temperature-gradients - and thus measured heat flow densities - change from place to place. This results in small gradients where the air flows into an insulation layer, and large gradients where the air flows out. So also here, the heatflow-profiles give an indirect picture of the airflow field.

When looking at pure rotative stack flow, there is no resulting airflow through the construction, which explains the existance of a 'neutral-axis', where pure conduction over the insulation layer exists.
At this axis, temperature falls linearly from hot box to cold box; here the conductive heatflows on both sides of the insulation are equal. Above the neutral axis, the conductive heatflow at the cold side of the insulation becomes higher then at the warm side; below the axis the opposite takes place.
This schedule results in the typical crossing lines of the heatflow profiles during stage 1 & 2 (small resulting airflow).

When looking at forced flow through air-open constructions (large resulting airflows), the temperature-gradient doesn't change with height, but diverges strongly with depth.
This results, during stage 3, in the large difference between the measured heatflows on the inside surface of the insulation, and the heatflows on the outside surface in field 1 & 2.

** Calculating local air velocities from measured heatflows (fig. 15)*

When taking convection into account (airflow from in- to outside), equation [1] changes into:

$$q = -\lambda.\frac{\partial T}{\partial x} - g_a.c_a.T \qquad [2]$$

Supposing stationary conditions, we can write the conservation law for heat transfer:

$$\frac{\partial q}{\partial x} = 0 \qquad [3]$$

Taking $\theta = \theta_{se}$ for $x = 0$
$\theta = \theta_{si}$ for $x = d$,
the temperature-curve over an insulation layer can be calculated:

$$\theta(x) = \frac{\theta_{si}.(1-e^{-\frac{Pe.x}{d}}) - \theta_{se}.(e^{-Pe} - e^{-\frac{Pe.x}{d}})}{1-e^{-Pe}} \qquad [4]$$

with $$Pe = \frac{g_a.c_a}{\frac{\lambda}{d}} \qquad [5]$$

By calculating the derivative of the temperature, the local conductive heatflow-curve is known:

$$q_{cond}(x) = -\lambda.\nabla\theta = -\frac{g_a.c_a.e^{-\frac{Pe.x}{d}}}{1-e^{-Pe}}.(\theta_{si}-\theta_{se}) \qquad [6]$$

Now, by introducing the material properties of the insulation layer and the measured temperatures on both surfaces in equation [6], and by plotting the relationship $q_{cond}(x) - q_{measured}$ as a function of g_a for the different measuring points (both $x = 0$ as $x = d$), we can find the local air velocities at both surfaces of the insulation layer for the different heights (fig 15). The intersection between the curves and the x-axis, marks the air velocity at which the theoretical conductive heatflow equals the measured one.
The values found are the velocity-components perpendicular to the roof-slope. With this calculation the implicit assumption is made that the air velocity at a given height through the insulation is a constant. This can only be judged correct if the velocity values found at both sides of the insulation are the same per height.
In field 1 and 2, the curves fit remarkably well, while in field 3 the velocities on the warm side of the insulation are systematically lower then those on the cold side.

** Local air-velocities (fig. 16)*

In figure 16, the averaged air-velocities through the insulation layer are plotted as a function of height. They give a good summary of the phenomena outlined higher.

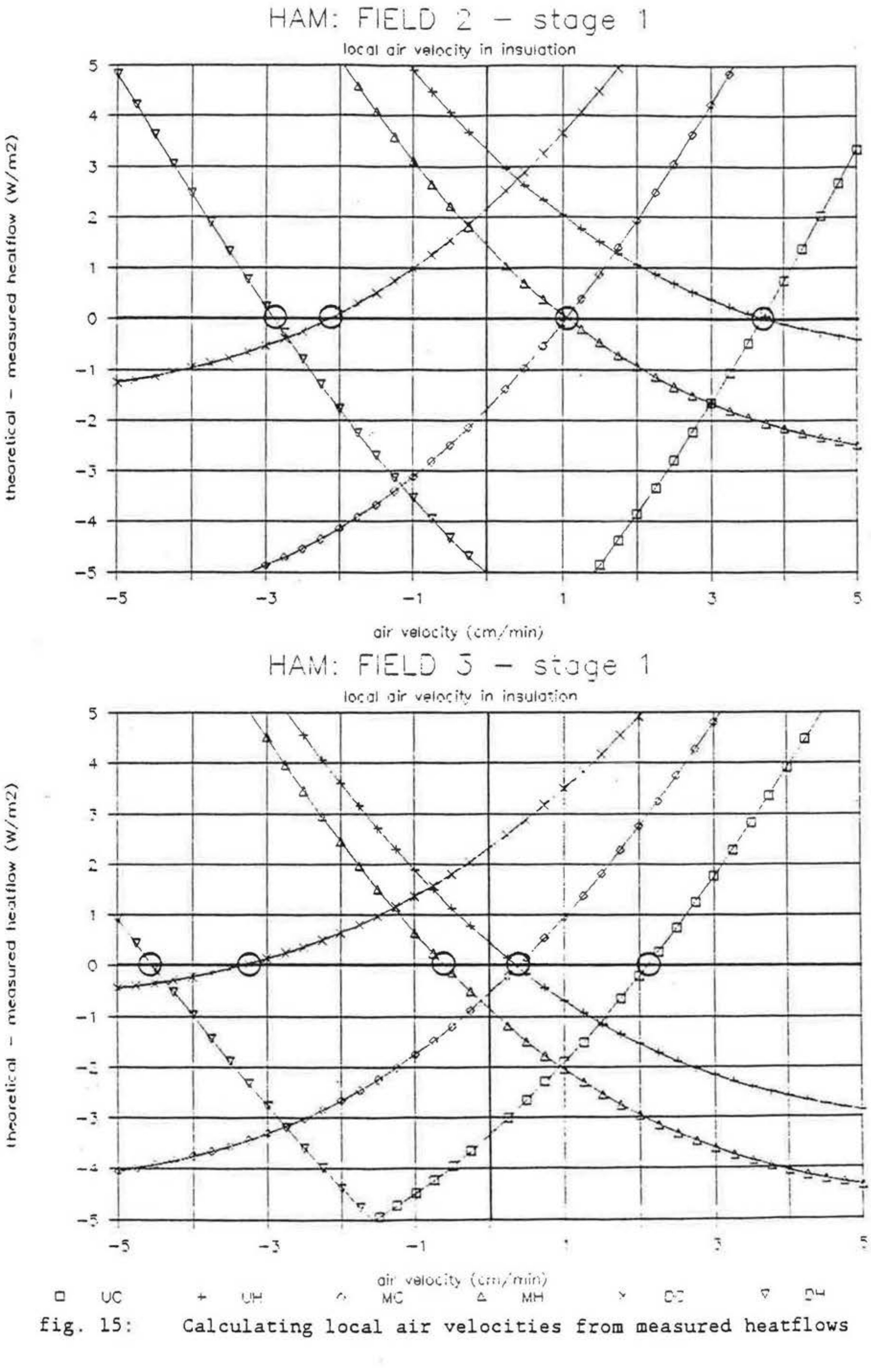

fig. 15: Calculating local air velocities from measured heatflows

fig. 16: Velocity profiles

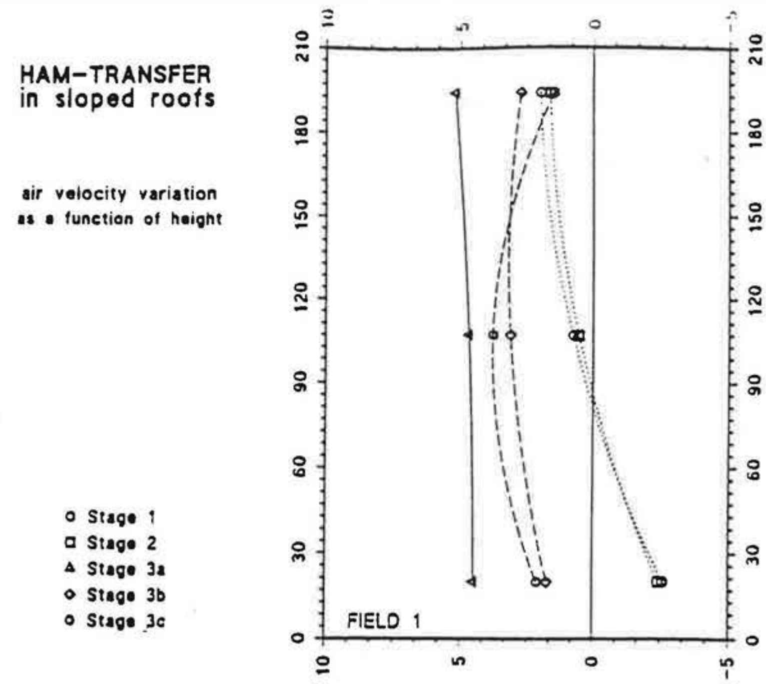

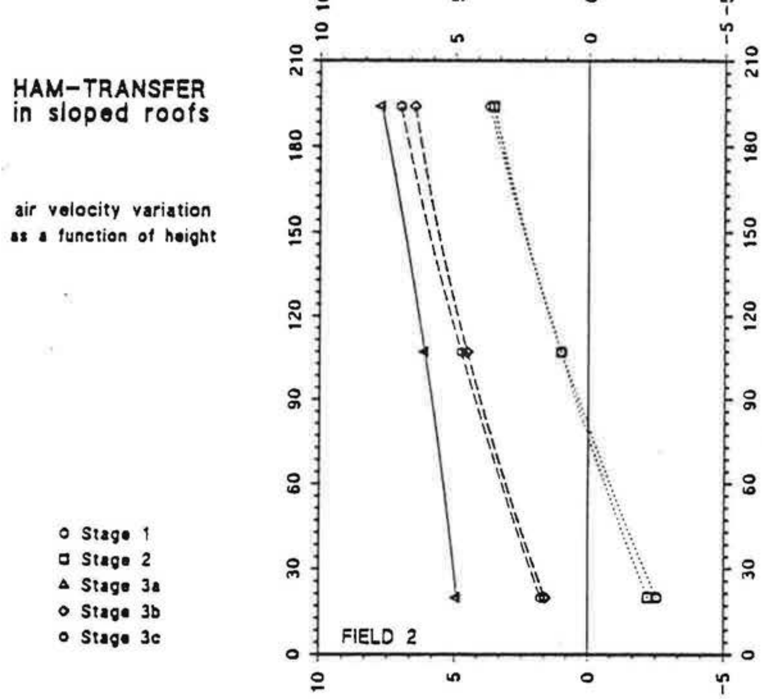

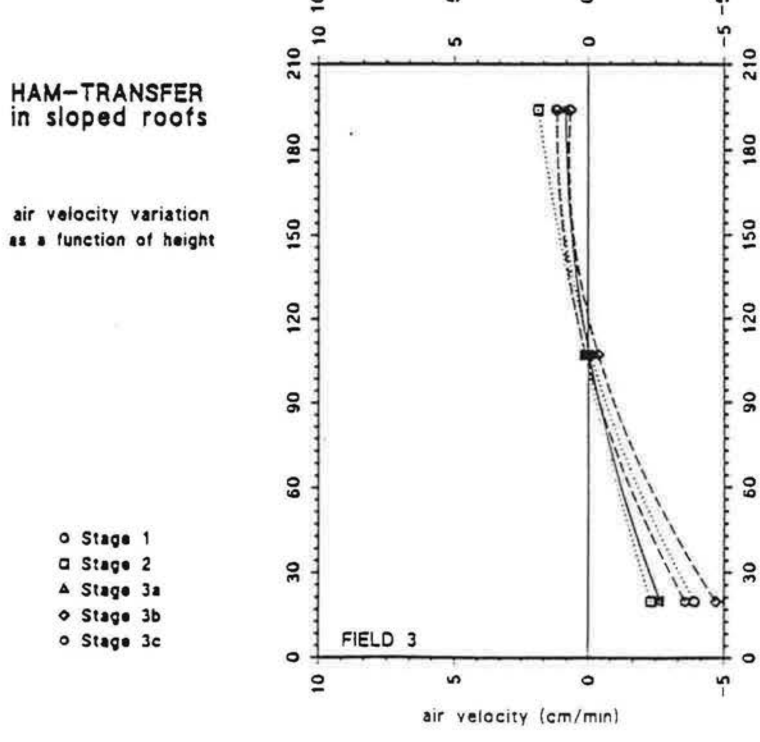

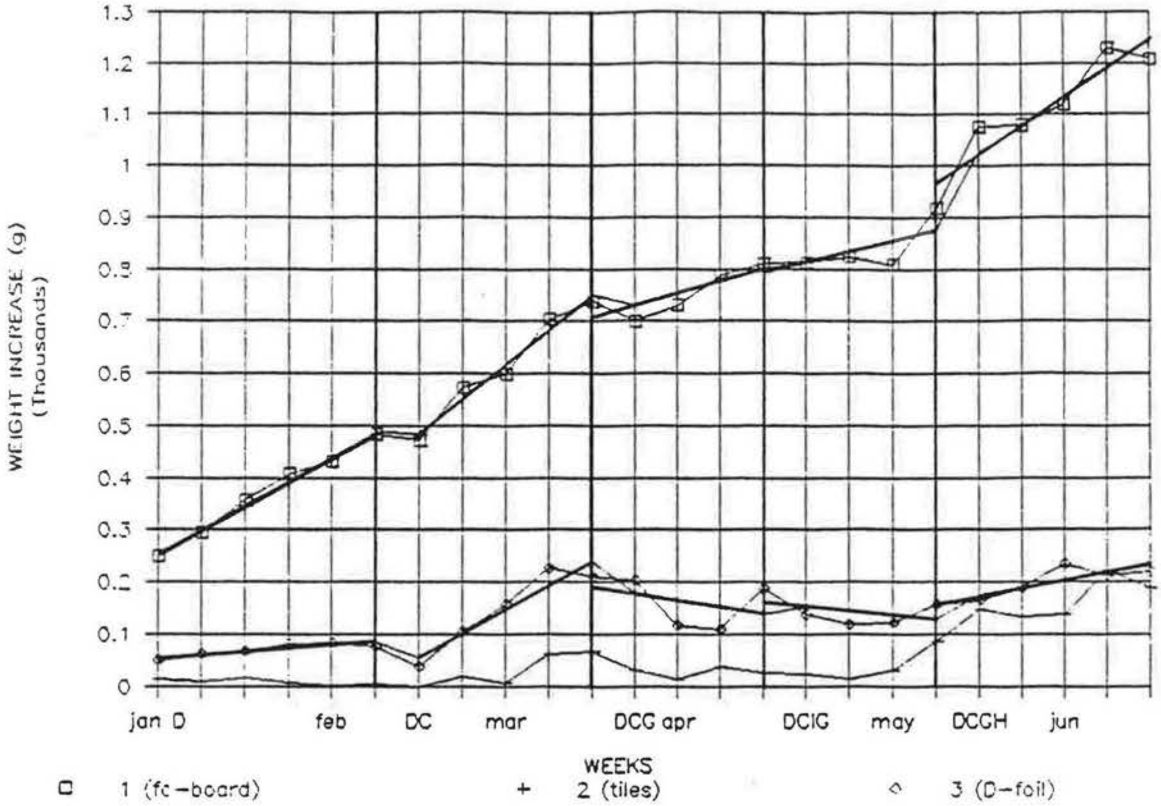

fig. 17: Weight increase in the underroofs vs time

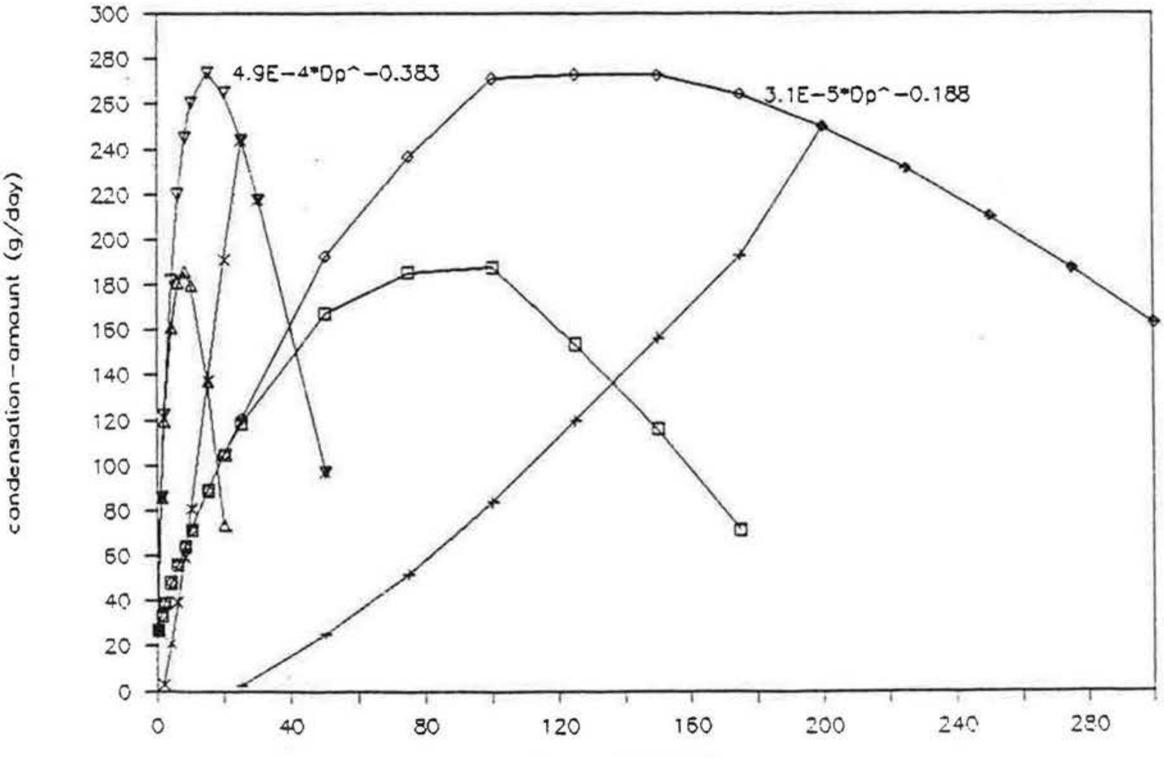

fig. 18: Condensation-flow rate vs air-pressure difference
K_a (GB) = 4.9E-4.$\Delta p^{-0.383}$: Δ underroofs x tiles ∇ sum
K_a (GB) = 3.1E-5.$\Delta p^{-0.188}$: □ underroofs + tiles ◊ sum

d. Moisture migration & condensation

* Underroofs (fig. 17)

Figure 17 shows the global weight increase of the 2 underroofs (field 1 & 3) during the 3 stages. The curves shown are the weekly weight increase of the underroof-frame, reduced with the weight increase of the frame (without underroof) in field 2, leaving the weight of the moisture absorbed by or condensated against the underroof itself.
The weight increase of the tile deck in field 2 (being the only possible condensation-plane) is also plotted.
A linear regression gives the following moisture flow rates per stage:

Table 2: moisture flow rate (g/day) per stage

place		st 1	st 2	st 3a	st 3b	st 3c
Field 1		6.6	9.5	3.3	3.0	8.1
underroof	σ =	0.3	1.0	1.4	1.7	1.5
Field 2		-0.3	2.5	-1.1	1.8	3.1
tiles	σ =	0.1	0.7	0.9	1.1	1.0
Field 3		0.9	6.6	-1.9	-1.1	2.0
underroof	σ =	0.2	1.3	2.3	1.4	0.6

Field 1: development
The underroof in field 1 is a fiber-cement board, a capillary-porous, highly hygroscopical material. Although this underroof increases a lot in weight during stage 1, no interstitial condensation occurs. During stage 2 the weight increases even more but only a little condensation-spot appears in the upper corner, not very alarming. Some mould starts growing around this spot and further on the upper half of the underroof. During stage 3a & b, from the moment the grooves are sawn in the gypsum board (resulting in high air flow rates through this construction), the weight increase stops and reaches a platform around 0.85 kg. Still a little condensation-spot and some mould are present around the same corner. It is only during stage 3b, when a severe vapour pressure-difference is installed, that the weight increases again. Now the condensation amounts enlarge: the upper half of the underroof is completely wet, with clear peaks on the top and around the overlap.

Field 3: development
The underroof of field 3, a micro-perforated, so called 'vapour-open', PE-foil, behaves completely different. During all the stages, interstitial condensation is clearly present, not homogeneously divided over the total surface, but with a pronounced peak against the upper half of the foil. The middle rafter of the field is marked as a dry(er) zone on the underroof. During stage 2, the water starts to drip down along the foil, creating local pools at the bottom of the measuring frame.
During stage 3a & b, the underroof-weight decreases a little, without ever making condensation disappear.

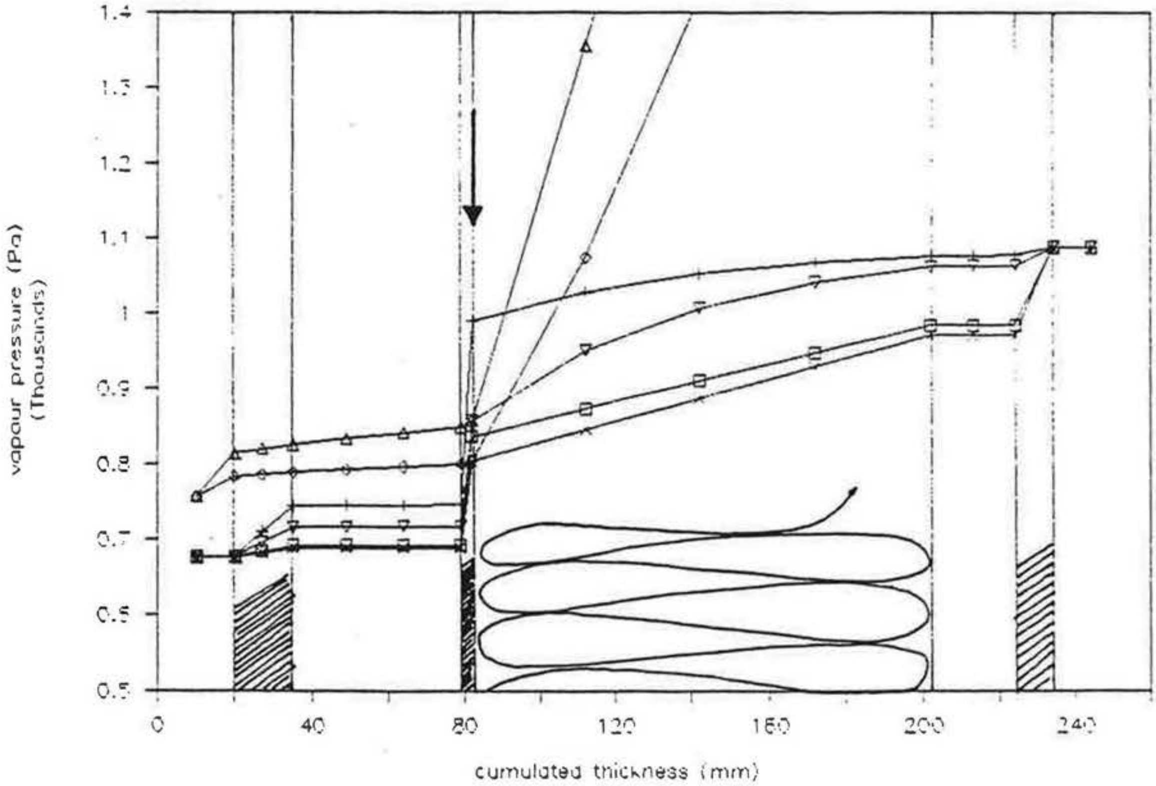

fig. 19: Typical vapour pressure-drop over field 1

Diffusion (Glazer) model: □ vapour pressure
◇ vapour saturation pressure
x adapted vapour pressure

Diffusion-Convection: + vapour pressure
Δ vapour saturation pressure
∇ adapted saturation pressure

Hygric behaviour: global interpretation

1. Natural and forced convection in and through a construction together with (2- or 3-dimensional) changes in geometry, make moisture migration and condensation **a local, non-homogeneous phenomenon**.

2. Forced convection from in- to outside makes the condensation behaviour of a construction **very sensitive to tiny changes** in air-openess or in boundary conditions.

   Opposite to diffusion, convection is a very quick phenomenon, able to transport larger amounts of moisture through a construction, and therefore being more important. When a moisted airflow in a construction meets a cold surface, the vapour will condensate against the surface, if the temperature of the surface is lower then the dewpoint of the air. The bigger the airflow rate, the more vapour reaches the cold surface, and the more striking the condensation amount becomes - at least as long as the surface temperature doesn't rise above the dew-point of the air.
   Indeed, airflow also creates enthalpee-flows, making the temperatures in the construction rise. Because the vapour pressures in a construction subjected to forced convection, become equal to the inside pressure very quickly, one can state: from the moment the airflow rate makes the surface-temperature rise above the dew-point of the inside air, condensation of moisted air on that surface becomes impossible.

   Fig. 18 shows this more clearly: here the condensation-flow rates as a function of the pressure difference are calculated for field 1, with a 1-dimensional analytical model, taking enthalpee- and latent heat-flow into account. The curves are plotted for two values of the air-permeance of the gypsum-board.
   Here also large condensation amounts on the tiles are predicted. Because of the high air-openess of the tile-deck however, and local air-flows around the tiles, this in fact never happens.
   In figure 19 a typical pressure-fall is compared with the pressure-course by diffusion.

   Former phenomenon makes condensation in air-open constructions very critical. A small change in air-permeance or an increase of the air pressure difference can either result in alarming condensation flow rates or in a **sudden** drying.
   During stage 3a & b, the grooves in the gypsum-board made the roofs seemly this air-open, that the condensation-peak already passed, resulting in lower condensation-flow rates and drying. Of course, the negative resulting airflow through field 3 pronounces this effect.

3. Also with convection, variations of the condensation-flow rate stay **directly dependant on variations of the vapour-pressure difference** (the air-flow rate being constant)

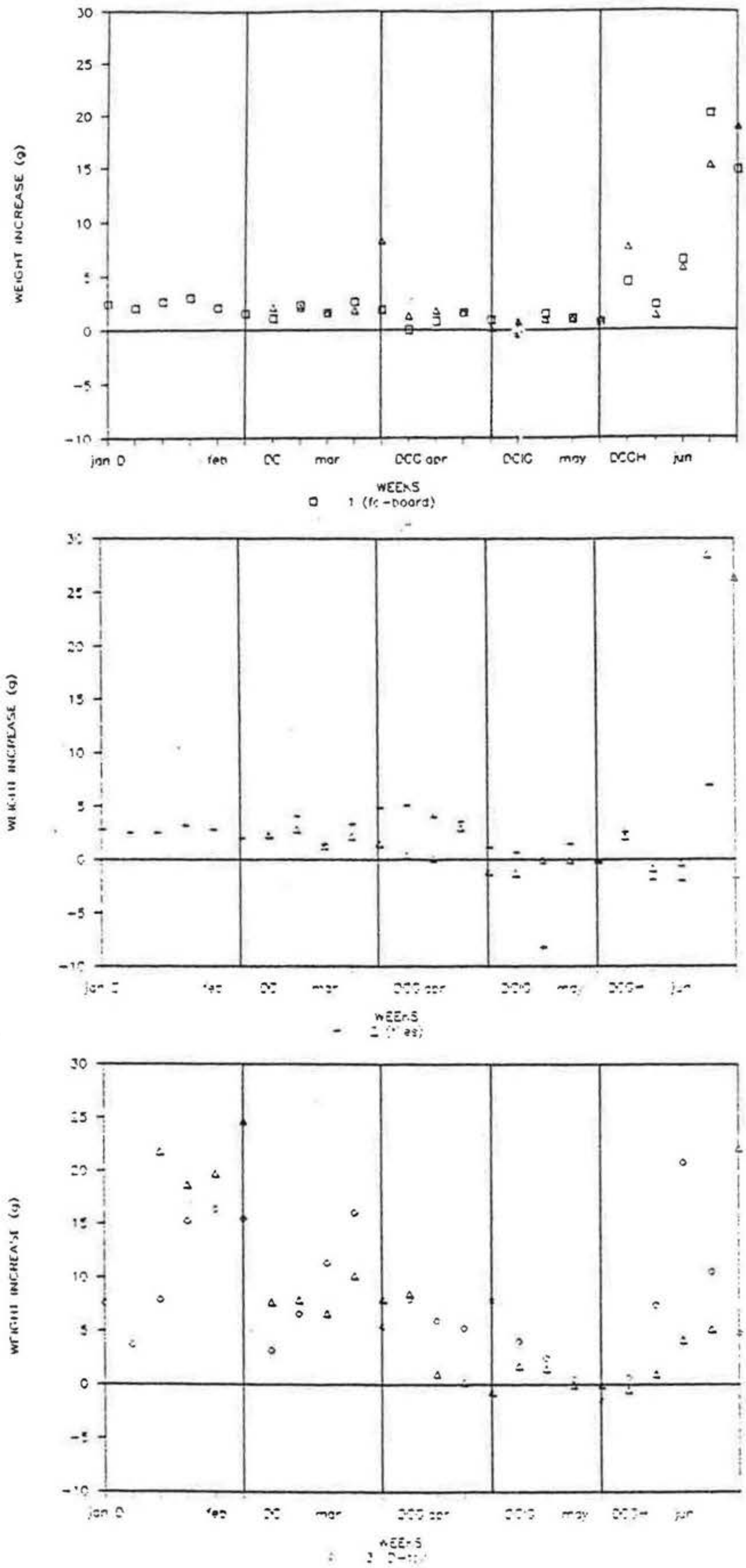

fig. 20: Weight increase of the insulation vs time

4. **Hygroscopicity** of the possible condensation-plane (field 1: the fiber-cement board) plays an important role in the hygric behaviour of the roof.

   Hygroscopicity plays a double role.
   The suction isotherm acts as moisture capacity and causes a slow rise of the moisture content of the material. Only if the whole pore-system is filled with water, the material being saturated, condensation can occur.
   The capacitive action of the underroof also creates a higher vapour pressure-gradient between inside climate and condensation-plane, resulting in a higher moisture flow rate to the underroof. This explains the bigger weight increase of the fiber-cement board.

   Suppose the moisture content of the board was 40 kg/m^3 (≈ hygroscopic moisture content at 50% RH), then the board can still absorb ± 1.7 kg water before it is completely saturated (w_{ca} = 358 kg/m^3).

<u>* Insulation (fig. 20)</u>

Development
The weight increase of the insulation follows the course of the condensation against the underroofs (field 1 & 3) or the tiles (field 2). Water, dripping off, can be seen as spread drops lying on the insulation, wettening the upper surface-layer. During the last stage, also more homogeneous tiny droplet fields were noticed in the upper surface-layer of the insulation of field 1 & 2. This might be caused by condensation, appearing in the insulation.

<u>* Tiles (fig. 21 - 22)</u>

Development
If condensation occurs against the tiles, it stays very local and starts in the tile-joints. In field 1 only in the upper row of the tile-deck some condensation droplets appear. Also little mould spots start growing around the joints of the upper tile-row. In field 2 condensation occurs during stage 2 & 3a, wettening the first 2, resp. 3 upper rows of the tile-deck. Here the condensation amount is the most pronounced of the 3 fields, but also stays very local. In field 3 no condensation can be noticed.
The air-openess of the tile-deck and the intensive mixing of cold box-air and cavity-air, explains why condensation against the tiles can not occur, or (in severe conditions) stays within a small range.

<u>* Laths and battens (fig. 23)</u>

These figures also are an illustration of the principles outlined above.

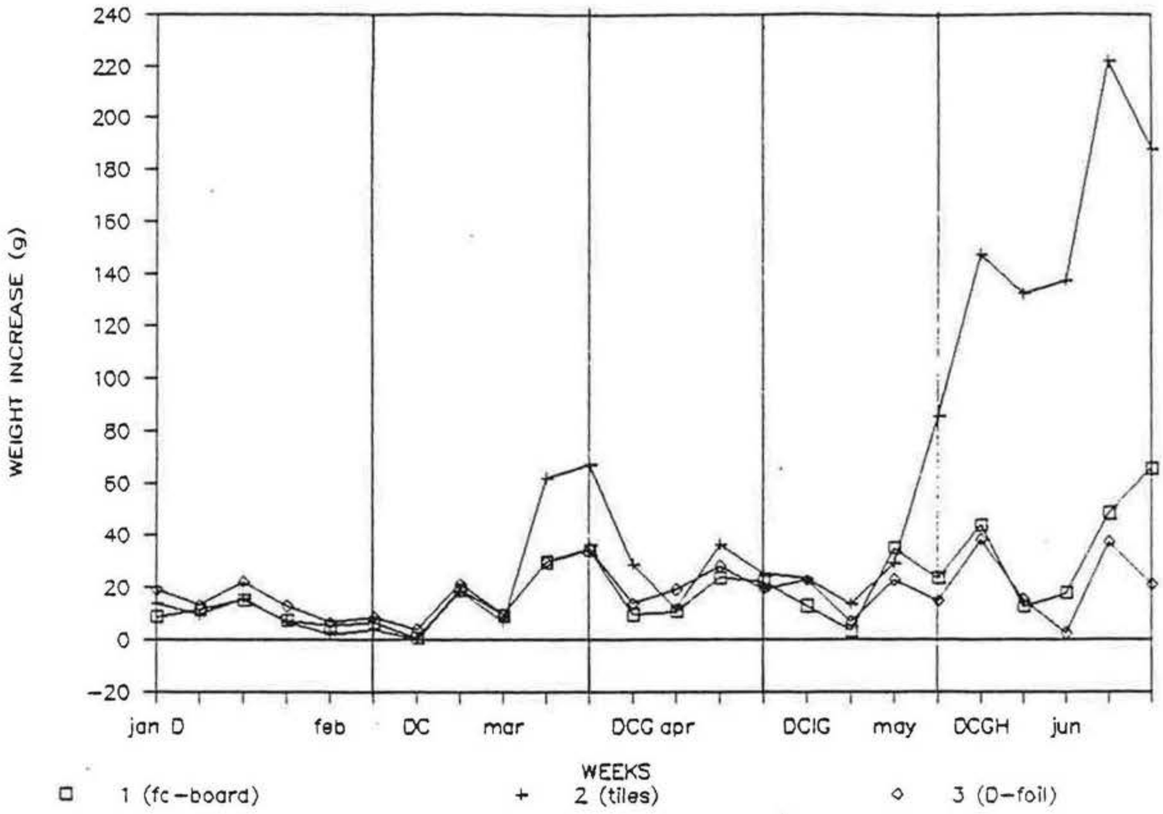

fig. 21: Weight increase of the tile-deck vs time

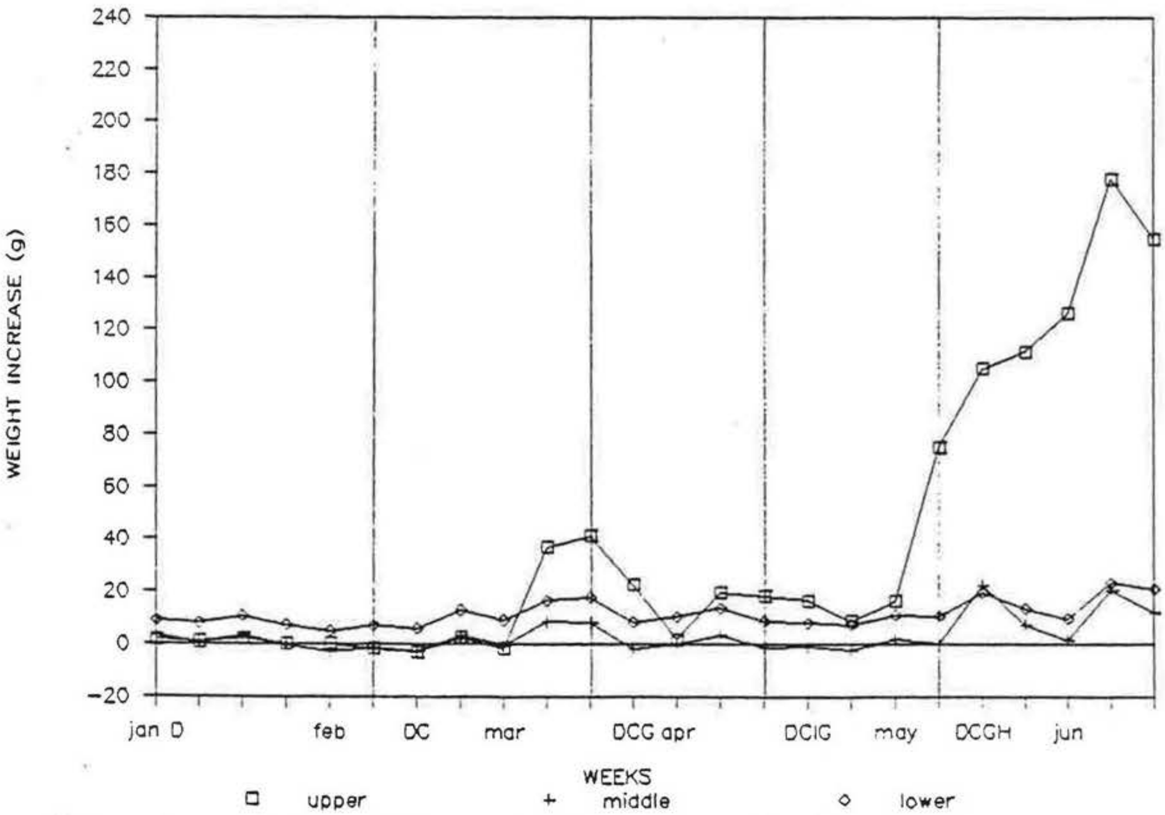

fig. 22: Weight increase of the tiles of field 2 vs time

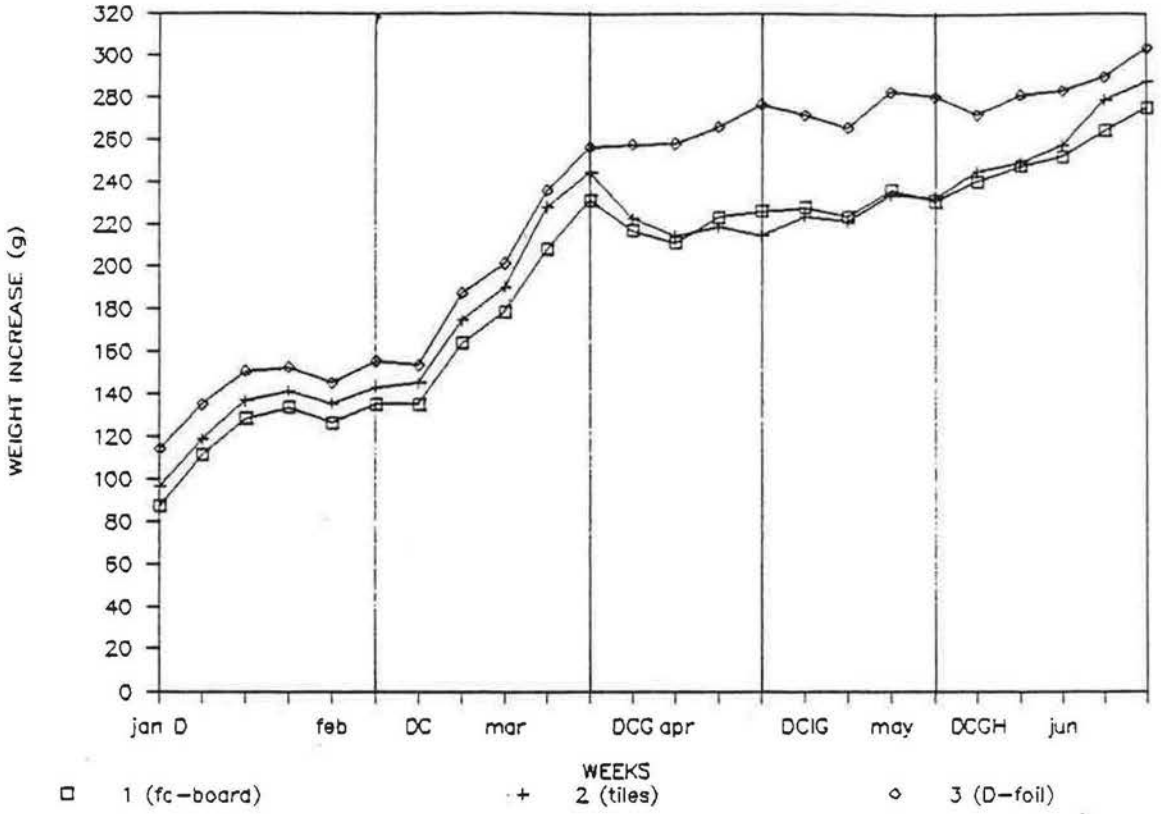

fig. 23: Weight increase of the laths and battens vs time

APPENDIX 1

- weekly averaged values of the boundary conditions
- boundary conditions, averaged per stage

AVERAGED BOUNDARY CONDITIONS DURING MEASURING PERIODS

STAGE	Th	Tc	Th-Tc	Ph	Td
1 (D)	20.2	2.8	17.5	1209.6	9.8
2 (DC)	23.4	3.0	20.4	1162.4	9.2
3a (DCG)	22.7	3.0	19.7	1088.6	8.2
3b (DCsG)	23.5	3.2	20.4	1179.2	9.4
3c (DCGh)	22.7	2.8	20.0	1398.0	12.0

STAGE	Pc	Ph-Pc	Pah-Pac	RVh	RVc
1 (D)	583.8	625.8	0.0	51.1	78.6
2 (DC)	660.2	502.2	18.3	40.1	87.2
3a (DCG)	677.0	411.6	2.6	39.3	89.6
3b (DCsG)	692.5	486.8	1.8	40.6	90.4
3c (DCGh)	675.5	722.5	1.7	50.6	90.6

BOUNDARY CONDITIONS FOR SLOPED TESTING ROOFS: WEEKLY AVERAGED

DATE	Th	Tc	Th-Tc	Ph	Pc	Ph-Pc	Pah	Pac	Pah-Pac	RVh	RVc
07-01	18.5	2.7	15.8	1117.5	572.9	544.6				52.6	77.4
14-01	21.2	2.9	18.3	1300.7	593.2	707.5				51.8	79.1
21-01	20.8	2.8	18	1242.1	588.4	653.7				50.6	78.8
28-01	20.5	2.8	17.7	1239.6	589.1	650.5				51.4	79.1
04-02	20.2	2.7	17.5	1202.8	580	622.8				50.7	78.4
11-02	20	2.6	17.4	1155.1	579.3	575.8				49.3	78.6
18-02	21.3	3.1	18.2	865.1	611.5	253.6				34.1	79.9
25-02	22.8	2.9	19.9	1104.5	637.2	467.3	14.4	-2.6	17	39.9	84.9
04-03	23.9	2.9	21	1219.3	662	557.3	16.2	-2	18.2	41.1	87.9
11-03	24.7	3.2	21.5	1329.9	695.5	634.4	17.2	-2.1	19.3	42.9	90.8
18-03	24.4	2.9	21.5	1293.1	694.9	598.2	16	-2.5	18.5	42.3	92.7
25-03	22.4	3.1	19.3	1073.5	705	368.5	5.6	2.1	3.5	39.7	92.5
01-04	21.7	2.9	18.8	905.9	679.5	226.4	-0.4	-3.1	2.7	34.9	90.4
08-04	23.1	2.9	20.2	1090.9	680.9	410	-0.2	-2.1	1.9	38.6	90.7
15-04	23.7	3.1	20.6	1284.2	642.6	641.6	0.9	-1.4	2.3	43.8	84.6
22-04	22.6	3	19.6	1060.1	683.3	376.8	1.7	-0.3	2	38.8	90.5
29-04	23.3	2.8	20.5	1102.3	665.9	436.4	2.3	1	1.3	38.5	89.1
06-05	23.4	3.3	20.1	1214.6	712.8	501.8	1.2	-0.2	1.4	42.3	92
13-05	24.8	3.5	21.3	1339.9	707.9	632	-0.3	-2.9	2.6	42.8	90
21-05	22.9	2.6	20.3	1347.6	656.6	691	2.7	0.2	2.5	48.3	89
27-05	22.5	2.9	19.6	1357.7	683.9	673.8	0.3	-1.5	1.8	49.9	91.1
03-06	23.1	2.8	20.3	1425.5	673.4	752.1	2.3	1	1.3	50.5	90.3
10-06	21.9	2.8	19.1	1334.1	669.3	664.8	1.4	0.1	1.3	51	89.7
17-06	23.3	2.8	20.5	1524.9	694.3	830.6	0.4	-1.3	1.7	53.2	92.7

APPENDIX 2

Per measuring point, per stage:

- averaged measured temperatures
- averaged measured heatflow densities
- calculated local air velocities

AVERAGED TEMPERATURES SLOPED ROOFS: STAGE 1

HEIGHT			194.00	150.50	107.00	63.50	20.00	AVG
FIELD 1	CB	0.00	2.78				2.68	2.73
D	TILc	5.00	3.03		3.20		2.90	3.04
	TILh	20.00	3.28		3.60		2.97	3.28
	UNRc	65.00	4.38		4.75		3.33	4.16
	INSc	68.00	7.93	4.60	6.48	4.10	3.42	5.31
	INSh	188.00	20.03	19.50	19.08	17.70	16.50	18.56
	GYPc	210.00	20.12		19.52		17.25	18.96
	GYPh	220.00	20.27		19.73		18.12	19.37
	HB	225.00	20.67		20.33		19.63	20.21
FIELD 2	CB		2.78				2.68	2.73
D	TILc		3.42					3.42
	TILh		4.47		3.10		3.07	3.54
	INSc		5.50	5.47	3.73	3.50	3.10	4.26
	INSh		19.95	19.60	18.90	17.53	16.38	18.47
	GYPc		20.05		19.30		17.43	18.93
	GYPh		20.15		19.65		18.37	19.39
	HB		20.64		20.33		19.63	20.20
FIELD 3	CB		2.78				2.68	2.73
D	TILc		2.87		2.85		2.87	2.86
	TILh		3.13		2.98		3.03	3.05
	UNRc		3.90		3.75		3.15	3.60
	INSc		6.00	4.05	4.32	3.52	3.17	4.21
	INSh		18.88	18.68	17.85	17.30	13.83	17.31
	GYPc		19.58		18.95		16.38	18.31
	GYPh		19.87		19.38		17.63	18.96
	HB		20.64		20.33		19.63	20.20

AVERAGED FLUXES

FIELD 1	INSc	(W/m2)	1.30	4.80	1.50
	INSh	(W/m2)	1.60	2.90	8.30
	Vc	(cm/min)	-2.50	0.8	-2.5
	Vh	(cm/min)	2.00	0.75	-2.70
FIELD 2	INSc	(W/m2)	11.60	6.20	1.70
	INSh	(W/m2)	0.90	3.00	8.90
	Vc	(cm/min)	3.70	1.00	-2.25
	Vh	(cm/min)	3.75	1.00	-2.86
FIELD 3	INSc	(W/m2)	7.10	4.50	0.80
	INSh	(W/m2)	3.30	4.80	10.10
	Vc	(cm/min)	2.10	0.40	-3.35
	Vh	(cm/min)	0.35	-0.60	-4.50

AVERAGED TEMPERATURES SLOPED ROOFS: STAGE 2

FIELD 1	CB	0.00	3.10				2.92	3.01
DC	TILc	5.00	3.58		3.66		3.38	3.54
	TILh	20.00	3.90		4.10		3.42	3.81
	UNRc	65.00	5.28		5.30		3.96	4.85
	INSc	68.00	9.26	5.22	6.10	4.98	4.14	5.94
	INSh	188.00	23.12	21.72	22.02	20.82	19.70	21.48
	GYPc	210.00	23.22		22.54		20.30	22.02
	GYPh	220.00	23.34		22.82		21.38	22.51
	HB	225.00	23.86		23.52		22.88	23.42
FIELD 2	CB		3.10				2.92	3.01
DC	TILc		4.18					4.18
	TILh		5.64		3.56		3.46	4.22
	INSc		7.62	6.02	3.78	4.08	3.58	5.02
	INSh		23.02	21.86	22.00	20.64	19.60	21.42
	GYPc		23.16		22.42		20.52	22.03
	GYPh		23.28		22.78		21.62	22.56
	HB		23.86		23.52		22.88	23.42
FIELD 3	CB		3.10				2.92	3.01
DC	TILc		3.36		3.24		3.18	3.26
	TILh		3.94		3.40		3.38	3.57
	UNRc		5.30		4.42		3.44	4.39
	INSc		7.00	5.26	5.36	4.14	3.96	5.14
	INSh		22.24	21.80	20.82	20.48	18.22	20.71
	GYPc		22.84		21.98		20.64	21.82
	GYPh		23.14		22.50		21.46	22.37
	HB		23.86		23.52		22.88	23.42

AVERAGED FLUXES

FIELD 1	INSc	(W/m2)	1.40	5.40	1.80	2.87
	INSh	(W/m2)	2.20	4.00	9.50	5.23
	Vc	(cm/min)	-2.75	0.5	-2.37	
	Vh	(cm/min)	1.63	0.60	-2.50	
FIELD 2	INSc	(W/m2)	12.30	7.60	2.30	
	INSh	(W/m2)	1.10	3.70	10.00	
	Vc	(cm/min)	3.65	1.12	-1.88	
	Vh	(cm/min)	3.50	1.00	-2.60	
FIELD 3	INSc	(W/m2)	9.20	5.90	2.10	
	INSh	(W/m2)	2.90	5.30	9.60	
	Vc	(cm/min)	2.50	0.80	-1.75	
	Vh	(cm/min)	1.25	-0.50	-2.90	

AVERAGED TEMPERATURES SLOPED ROOFS: STAGE 3a

FIELD 1	CB	0.00	3.10				2.90	3.00
DCG	TILc	5.00	3.80		4.18		3.78	3.92
	TILh	20.00	4.25		5.40		4.18	4.61
	UNRc	65.00	6.48		8.30		6.08	6.95
	INSc	68.00	12.98	6.53	8.78	8.08	7.95	8.86
	INSh	188.00	22.78	23.13	22.53	22.43	21.85	22.54
	GYPc	210.00	22.75		22.43		20.63	21.93
	GYPh	220.00	22.83		22.58		22.03	22.47
	HB	225.00	23.13		22.88		22.20	22.73
FIELD 2	CB		3.10				2.90	3.00
DCG	TILc		5.03					5.03
	TILh		8.38		4.35		4.25	5.66
	INSc		10.45	10.20	5.80	9.00	6.73	8.44
	INSh		22.75	22.98	22.53	22.80	22.05	22.62
	GYPc		22.80		21.60		22.08	22.16
	GYPh		22.78		22.63		22.23	22.54
	HB		23.13		22.88		22.20	22.73
FIELD 3	CB		3.10				2.90	3.00
DCG	TILc		3.40		3.23		3.18	3.27
	TILh		3.80		3.35		3.30	3.48
	UNRc		4.85		4.23		3.43	4.17
	INSc		6.30	4.83	4.93	4.08	3.90	4.81
	INSh		21.35	21.63	20.33	19.85	16.95	20.02
	GYPc		22.08		21.40		19.58	21.02
	GYPh		22.38		21.88		20.38	21.54
	HB		23.13		22.88		22.20	22.73

AVERAGED FLUXES

FIELD 1	INSc	(W/m2)	2.10	10.80	14.50	9.13
	INSh	(W/m2)	0.30	0.30	0.80	0.47
	Vc	(cm/min)	-0.76	3.6	5.1	
	Vh	(cm/min)	5.20	5.80	3.90	
FIELD 2	INSc	(W/m2)	19.40	20.60	17.80	
	INSh	(W/m2)	0.10	0.30	0.80	
	Vc	(cm/min)	7.85	6.05	5.70	
	Vh	(cm/min)	7.63	6.20	4.12	
FIELD 3	INSc	(W/m2)	6.90	4.80	2.00	
	INSh	(W/m2)	4.00	5.00	10.20	
	Vc	(cm/min)	1.45	0.25	-1.75	
	Vh	(cm/min)	0.20	-0.30	-3.60	

AVERAGED TEMPERATURES SLOPED ROOFS: STAGE 3b

FIELD 1	CB	0.00	3.23				3.05	3.14
DC1G	TILc	5.00	3.68		4.03		3.60	3.77
	TILh	20.00	3.98		5.00		3.78	4.25
	UNRc	65.00	5.40		7.45		5.18	6.01
	INSc	68.00	10.10	5.33	9.00	5.93	5.98	7.27
	INSh	188.00	23.40	23.15	23.00	22.38	21.83	22.75
	GYPc	210.00	23.20		23.05		22.15	22.80
	GYPh	220.00	23.55		23.28		22.43	23.08
	HB	225.00	24.00		23.65		22.90	23.52
FIELD 2	CB		3.23				3.05	3.14
DC1G	TILc		4.50					4.50
	TILh		7.00		4.05		3.90	4.98
	INSc		8.65	8.68	4.95	5.40	5.15	6.57
	INSh		23.45	23.70	23.20	23.40	21.95	23.14
	GYPc		23.53		23.30		22.10	22.98
	GYPh		23.55		23.35		22.60	23.17
	HB		24.00		23.65		22.90	23.52
FIELD 3	CB		3.23				3.05	3.14
DC1G	TILc		3.40		3.35		3.33	3.36
	TILh		3.73		3.45		3.43	3.53
	UNRc		4.73		4.25		3.50	4.16
	INSc		6.00	4.88	5.08	3.98	3.63	4.71
	INSh		21.98	21.83	20.98	20.05	16.10	20.19
	GYPc		22.80		22.10		19.15	21.35
	GYPh		23.18		22.60		20.68	22.15
	HB		24.00		23.65		22.90	23.52

AVERAGED FLUXES

FIELD 1	INSc	(W/m2)	1.60	9.70	8.70	6.67
	INSh	(W/m2)	1.30	1.10	2.80	1.73
	Vc	(cm/min)	-2.25	3.05	2.1	
	Vh	(cm/min)	2.75	3.25	1.37	
FIELD 2	INSc	(W/m2)	18.70	17.70	9.30	
	INSh	(W/m2)	0.20	0.80	3.30	
	Vc	(cm/min)	6.25	4.65	2.12	
	Vh	(cm/min)	6.75	4.45	1.10	
FIELD 3	INSc	(W/m2)	6.90	4.50	0.70	
	INSh	(W/m2)	4.60	5.30	13.90	
	Vc	(cm/min)	1.25	-0.15	-4.00	
	Vh	(cm/min)	0.10	-0.60	-5.40	

AVERAGED TEMPERATURES SLOPED ROOFS: STAGE 3c

FIELD 1	CB	0.00	2.94				2.76	2.85
DC1GH	TILc	5.00	3.48		3.96		3.34	3.59
	TILh	20.00	3.94		4.94		3.52	4.13
	UNRc	65.00	5.50		7.96		4.70	6.05
	INSc	68.00	9.34	5.30	10.26	6.26	5.82	7.40
	INSh	188.00	22.48	22.36	22.36	21.88	21.40	22.10
	GYPc	210.00	22.26		22.44		19.82	21.51
	GYPh	220.00	22.70		22.54		21.76	22.33
	HB	225.00	23.22		22.88		22.14	22.75
FIELD 2	CB		2.94				2.76	2.85
DC1GH	TILc		4.22					4.22
	TILh		6.16		3.76		3.52	4.48
	INSc		8.08	8.24	4.56	4.56	4.64	6.02
	INSh		22.72	22.92	22.42	22.60	21.18	22.37
	GYPc		22.76		22.50		21.34	22.20
	GYPh		22.78		22.58		21.84	22.40
	HB		23.22		22.88		22.14	22.75
FIELD 3	CB		2.94				2.76	2.85
DC1GH	TILc		3.23		3.10		3.05	3.13
	TILh		3.68		3.25		3.15	3.36
	UNRc		4.90		4.20		3.43	4.18
	INSc		6.00	4.85	5.15	3.83	3.58	4.68
	INSh		21.30	21.10	20.48	19.28	16.08	19.65
	GYPc		22.00		21.33		17.98	20.43
	GYPh		22.30		21.80		19.98	21.36
	HB		23.22		22.88		22.14	22.75

AVERAGED FLUXES

FIELD 1	INSc	(W/m2)	2.00	10.90	10.10	7.67
	INSh	(W/m2)	2.20	0.90	2.60	1.90
	Vc	(cm/min)	-1.75	4.25	2.75	
	Vh	(cm/min)	1.50	3.37	1.50	
FIELD 2	INSc	(W/m2)	21.70	19.90	10.70	
	INSh	(W/m2)	0.20	1.00	3.60	
	Vc	(cm/min)	7.37	5.40	2.75	
	Vh	(cm/min)	6.70	4.15	0.80	
FIELD 3	INSc	(W/m2)	7.90	5.20	1.40	
	INSh	(W/m2)	3.80	4.90	12.10	
	Vc	(cm/min)	1.86	0.46	-2.52	
	Vh	(cm/min)	0.45	-0.26	-4.63	

REFERENCES

1. Hens H., Uytterhoeven W., Vaes F., Neyrinckx L., Globale vochtgedrag van hellende daken (Overall moisture behaviour of sloped roofs), Rapport onderzoek WTCB- KU Leuven - IWONL, conventie 3687, 1983, 82 pp
2. Hens H., Lecompte J., Mulier G., Staelens P., Globale vochtgedrag van hellende daken (Overall moisture behaviour of sloped roofs), Rapport onderzoek WTCB - KU Leuven - IWONL, conventie 4213, 1986, 94 pp
3. Lecompte J., De invloed van natuurlijke convectie op de thermische kwaliteit van geïsoleerde spouwconstructies (The influence of the stack effect on the thermal quality of insulated cavity constructions) Doctoraal proefschrift, KU Leuven, 1989, 206 pp
4. Hens H., The hygrothermal behaviour of sloped roofs, CIB W40 'Heat and moisture transfer in buildings', 1989, 16 pp
5. Laboratorium Bouwfysica, KU leuven, Rapport 90/11, 1990, 12 pp.
6. Hens H., Modelling heat-air-moisture transfer in and through construction parts, paper, 9 pp
7. Hens H., The hygro-thermal behaviour of sloped roofs, paper, 11 pp
8. IEA-Annex 14, Condensation and energy, Volume 1, Sourcebook, Acco Leuven, 1991
9. IEA-Annex 14, Condensation and energy, Volume 3, Catalogue of Material Properties, Acco Leuven, 1991
10. De Groeve A., Van Lokeren D., Hellende daken met isolatie in het dakschild: inwendige kondensatie ten gevolge van diffusie en convectie (Sloped roofs with side-insulation: interstitial condensation caused by diffusion and convection), eindverhandeling, KIH Oost-Vlaanderen, Gent, 1991, 103 pp